

## RESEARCH ARTICLE

# Bioactive potentiality of secondary metabolites from endophytic bacteria against SARS-COV-2: An *in-silico* approach

Yasmin Akter<sup>1‡</sup>, Rocktim Barua<sup>1‡</sup>, Md. Nasir Uddin<sup>1</sup>, Abul Fazal Muhammad Sanullah<sup>2</sup>, Lolo Wal Marzan<sup>1\*</sup>

**1** Department of Genetic Engineering and Biotechnology, Faculty of Biological Sciences, University of Chittagong, Chittagong, Bangladesh, **2** Department of Chemistry, Faculty of Sciences, University of Chittagong, Chittagong, Bangladesh

‡ These authors contributed equally to this work and share the first authorship.

\* [marzan.geb@cu.ac.bd](mailto:marzan.geb@cu.ac.bd)



## OPEN ACCESS

**Citation:** Akter Y, Barua R, Nasir Uddin M., Muhammad Sanullah AF, Marzan LW (2022) Bioactive potentiality of secondary metabolites from endophytic bacteria against SARS-COV-2: An *in-silico* approach. PLoS ONE 17(8): e0269962. <https://doi.org/10.1371/journal.pone.0269962>

**Editor:** Milkyas Endale, Adama Science and Technology University, ETHIOPIA

**Received:** January 22, 2022

**Accepted:** May 31, 2022

**Published:** August 4, 2022

**Peer Review History:** PLOS recognizes the benefits of transparency in the peer review process; therefore, we enable the publication of all of the content of peer review and author responses alongside final, published articles. The editorial history of this article is available here: <https://doi.org/10.1371/journal.pone.0269962>

**Copyright:** © 2022 Akter et al. This is an open access article distributed under the terms of the [Creative Commons Attribution License](https://creativecommons.org/licenses/by/4.0/), which permits unrestricted use, distribution, and reproduction in any medium, provided the original author and source are credited.

**Data Availability Statement:** We declare that our manuscript data are fully available without restriction.

## Abstract

Five endophytic bacterial isolates were studied to identify morphologically and biochemically, according to established protocols and further confirmed by 16S rDNA Sanger sequencing, as *Priestia megaterium*, *Staphylococcus caprae*, *Neobacillus drentensis*, *Micrococcus yunnanensis*, and *Sphingomonas paucimobilis*, which were then tested for phytohormone, ammonia, and hydrolytic enzyme production. Antioxidant compounds total phenolic content (TPC), and total flavonoid content (TFC) were assessed by using bacterial crude extracts obtained from 24-hour shake-flask culture. Phylogenetic tree analysis of those identified isolates shared sequence similarities with the members of *Bacillus*, *Micrococcus*, *Staphylococcus*, and *Pseudomonas* species, and after GenBank submission, accession numbers for the nucleotide sequences were found to be MW494406, MW494408, MW494401, MW494402, and MZ021340, respectively. *In silico* analysis was performed to identify their bioactive genes and compounds in the context of bioactive secondary metabolite production with medicinal value, where nine significant bioactive compounds according to six different types of bioactive secondary metabolites were identified, and their structures, gene associations, and protein-protein networks were analyzed by different computational tools and servers, which were reported earlier with their antimicrobial, anti-infective, antioxidant, and anti-cancer capabilities. These compounds were then docked to the 3-chymotrypsin-like protease (3CL<sup>PRO</sup>) of the novel SARS-COV-2. Docking scores were then compared with 3CL<sup>PRO</sup> reference inhibitor (lopinavir), and docked compounds were further subjected to ADMET and drug-likeness analyses. Ligand-protein interactions showed that two compounds (microansamycin and aureusimine) interacted favorably with coronavirus 3CL<sup>PRO</sup>. Besides, *in silico* analysis, we also performed NMR for metabolite detection whereas three metabolites (microansamycin, aureusimine, and stenothricin) were confirmed from the 1H NMR profiles. As a consequence, the metabolites found from NMR data aligned with our *in-silico* analysis that carries a significant outcome of this research. Finally, Endophytic bacteria collected from medicinal plants can provide new leading bioactive compounds against target proteins of SARS-COV-2, which could be an effective approach to accelerate drug innovation and development.

**Funding:** The author(s) received no specific funding for this work.

**Competing interests:** The authors have declared that no competing interests exist.

## Introduction

Endophytes are symbiotic microorganisms that thrive in seemingly healthy interior plant tissues without causing any harm to the host plants, and they are mostly bacterial and fungal species [1]. Mutualism has become synonymous with endophytes, as both hosts and microorganisms exhibit a synergistic relationship with each other. To date, the symbiotic interaction between plants and endophytes appears to be beneficial to both sides: it benefits the endophyte by increasing the availability of the plant's nutrients [2], and it benefits the plant by providing pathogen protection, improving nutrient uptake, promoting plant growth, and stress tolerance [1–3]. Natural compounds from endophytes exhibit activity as antimicrobials, antifungals, anticarcinogens, immunosuppressants, or antioxidants [4]; thus, secondary metabolites produced by endophytes can be implemented as therapeutics in the pharmaceutical and agricultural industries [3]. Endophytes have been linked to more than 200 genera from 16 phyla of bacteria [5], with the majority of the species belonging to the phyla Proteobacteria (90%) and most regularly Firmicutes and Actinobacteria [6, 7]. The diversity of endophytic bacteria ranges from gram-positive to gram-negative bacteria throughout all ecosystems [8]. Bacterial endophytes occupy an ecological niche comparable to phytopathogens, making them good candidates for biocontrol agents. Plant growth-promoting (PGP) endophytes have favorable influences on plant growth because of their metabolic activity and functional variety [7, 9]. They promote plant growth by developing symbiotic relationships, nitrogen fixation, phosphate solubilization, and the generation of important phytohormones such as indole acetic acid (IAA), abscisic acid, cytokinin, and others [10, 11]. Secondary metabolites are organic chemicals produced by plants, bacteria, or fungi that are not directly involved in the organism's regular growth, development, or reproduction, known as specialized metabolites, toxins, secondary products, or natural products [12]. It is not required for bacteria to flourish, but it does help them to interact more effectively with their environment. Bacterial endophytes produce terpenoids, alkaloids, polyketides, nonribosomal peptides (NRPs), phenols, enzymes, and phytohormones that aid plant-bacteria interactions and colonization.

Endophytic bacteria from medicinal plants offer the possibility of discovering a wide range of chemicals as well as a sustainable source of natural products. It has been reported that in medicinal plants, Bacillales, Enterobacterales, and Pseudomonadales were the most prevalent orders, accounting for 72.62% of the total, and *Bacillus*, *Pantoea*, and *Pseudomonas* were the most prevalent genera, accounting for 58.92%. *Bacillus*, *Pseudomonas*, and *Paenibacillus* can influence the growth, stress resistance, and metabolism of medicinal plants, and *Streptomyces* has been observed to promote plant growth and development [13]. Surfactin, Iturin, Fengycin, Munumbicins, and many more bioactive compounds with anti-infective, antimicrobial, anti-cancer, and anti-inflammatory bioactive compounds have been purified from various medicinal plants throughout the world [14].

Genome sequencing, comparative genomics, microarray, next-generation sequencing, metagenomics, and metatranscriptomics are some of the techniques utilized or that can be employed in modern endophytic research to unravel the plant–endophyte connection. Through the genome mining approach, the genetic characteristics that directly or indirectly govern diverse bioactivities, as well as putative bioactive secondary metabolites, have been discovered. It helps to identify specific genes involved in antibiotic resistance mechanisms, antibiotic synthesis, plant growth promotion, the endophytic secretory system, surface attachment and insertion elements, the transport system, and other metabolic systems [15]. On the other hand, comparative multigenome analysis is very useful in understanding the genetic and metabolic diversity of comparable or related microorganisms that interact with plants and animals in various ways [16]. To identify the gene clusters (smBGCs) for the secondary metabolite

biosynthetic pathways in the genome, several bioinformatics tools have been established, including BAGEL [17], ClustScan, CLUSEAN [18], NP searcher, PRISM [15], and antiSMASH [19]. The smBGC database has been set up to aid the search for known and novel metabolites that can be linked to traditional ways of characterizing molecules through chromatography and spectroscopy. Currently, *in silico* analysis has created a junction to predict and validate laboratory and computerized analyses [20].

Microbial secondary metabolites (MSMs) have been utilized to synthesize novel medicines to treat a variety of pathogens, including viruses, bacteria, fungi, and parasites, since they are simple and dependable sources [21, 22]. These secondary metabolites can be detected by different techniques such as NMR, GC, LC, CE etc [23]. Nuclear magnetic resonance (NMR) spectroscopy has been recognized as a reliable method that frequently applied in metabolomics studies [24]. A variety of metabolites can be identified by using <sup>1</sup>H NMR spectroscopy as well as different bioactive antiviral compounds [25].

The antiviral bioactive compounds isolated from different bacteria are listed in **Table 1**. The recent pandemic officially known as coronavirus disease 2019 (COVID-19) is caused by a novel coronavirus known as severe acute respiratory syndrome coronavirus 2 (SARS-COV-2) that poses a threat to global public health.

It was initially detected in December 2019 in Wuhan, China [26], and on 11 March 2020, the outbreak was declared by the World Health Organization (WHO) as a global pandemic that has caused a total death of 4,644,740 worldwide as of September 15, 2021, with nearly 4 million new cases reported globally in the past week (6–12 September) according to the World Health Organization. Most *in silico* research is ongoing around the world to identify anti-SARS-COV-2 drugs of either microbial or plant origins. Diversified microbial metabolites have been depicted to represent promising antiviral activity against a variety of DNA and RNA viruses, which is turning to an emerging trend for therapeutic applications of microbial metabolites as antiviral agents [27]. Therefore, metabolites produced by endophytic microorganisms might act as an emerging source of antiviral bioactive compound [1, 28–30]. Molecular docking and other computing approaches have been useful in the first large-scale screening of numerous natural chemicals and small molecules that directly inhibit critical target proteins in this direction. Reports on virtual screening of current

**Table 1. Antiviral bioactive compounds isolated from bacteria.**

Microorganisms	Antiviral compounds	Group	Virus/Disease
<i>Streptomyces avermitilis</i>	Avermectin B1a	Lactone	NR
<i>E. coli</i>	Baicalein	Lactone	DENV-2, SARS-COV2
<i>E. coli</i>	Scutellarein	Lactone	SARS-COV
<i>E. coli</i>	Rosmarinic acid	Lactone	HCV, HIV
<i>Lactobacillus sp</i>	Exopolysaccharide	Polysaccharide	Adenovirus
<i>Streptomyces koyangensis</i>	Neoabyssomicin D	Polyketone	HSV
<i>Streptomyces sp</i>	Antimycin A	NR	Western equine encephalitis virus
<i>Streptomyces roseus</i>	Leupeptin	Peptide	Marburg virus
<i>Bacillus licheniformis</i>	Exopolysaccharide	Polysaccharide	HSV1
<i>Myxococcus stipitatus</i>	Phenalamide	Peptide	HIV-1
<i>Bacillus pumilus</i>	Pumilacidins A-G	Peptide	HSV1
<i>Labilithrix luteola</i>	Labindoles A; Labindoles B	NR	HCV

**Note:** HIV: Human immunodeficiency virus; HSV: Herpes simplex virus, HCV: Hepatitis C virus, DENV: Dengue virus, SARS-COV: Severe acute respiratory syndrome coronavirus

<https://doi.org/10.1371/journal.pone.0269962.t001>

antiviral medicines based on known knowledge of SARS-COV-2 and closely similar coronaviruses, available databases and natural agents against emerging targets such as viral spike proteins, envelope protein, protease, nucleocapsid protein, and 3CL hydrolase are rapidly emerging [31–33]. The 3-chymotrypsin-like protease (3CL<sup>PRO</sup>), which is well known as the main protease (M<sup>PRO</sup>), and the papain-like protease (PL<sup>PRO</sup>) of the virus are two proteases vital to transcription and replication of the proteins encoded by the viral genome due to their peculiarity in splitting the two translated polyproteins (PP1a and PP1ab) into separate functional constituents [34]. A variety of flavonoids have been reported to have antiviral activity against SARS-COV by inhibiting 3C-like protease (3CL<sup>PRO</sup>) [35], where the 3CL<sup>PRO</sup> of COVID-19, which is known as the main protease, depicted 96% sequence similarity with that of SARS-COV [36]. As the autocleavage process is very important for viral propagation, 3CL<sup>PRO</sup> acts as an excellent drug target for anti-coronaviral infection. Therefore, 3CL<sup>PRO</sup> can be considered an excellent drug target, and many efforts have been assigned to its study, as it has a key role in the replication cycle [33].

Therefore, the aims of the present study are to isolate and characterize endophytic bacteria from different parts of medicinal plants, evaluate their plant growth-promoting and antioxidant properties, predict and detect their secondary metabolites and analyze bioactive metabolites as potential antiviral compounds against SARS-COV-2.

## Materials and methods

### Sample collection

A total of 16 fresh and healthy medicinal plants were collected from the University of Chittagong campus (Table 2) into sterile zipper bags and then labeled and sealed. The samples were then immediately transferred to the lab maintaining a cold chain and stored in a 4°C refrigerator for further processing.

**Table 2. List of collected medicinal plant samples and their collection areas.**

Serial No.	Date of Collection	Season	Name of Plants	Location (Around CU campus)	Types of Plants	Plant Parts Used	Isolate code
1	15/07/2019	Rainy	<i>Ocimum tenuiflorum</i> (তুলসী)	1 no. Gate	Herb	L, R, S	TL, TR, TS
2	18/07/2019	Rainy	<i>Eclipta prostrata</i> (কালসোনা)	Science Faculty	Herb	L, R, S	KL, KR, KS
3	28/07/2019	Rainy	<i>Justicia adhatoda</i> (বাসক)	Central Mosque	Shrub	L, R, S	BL, BR, BS
4	03/08/2019	Rainy	<i>Clerodendrum viscosum</i> (ভাট)	Biol. Sci. Faculty	Shrub	L, R, S	VL, VR, VS
5	03/08/2019	Rainy	<i>Leonurus sibiricus</i> (দ্রোণপুষ্প)	Biol. Sci. Faculty	Herb	L, R, S	DL, DR, DS
6	03/08/2019	Rainy	<i>Melastoma malabathricum</i> (দাঁতরাঙা)	Biol. Sci. Faculty	Shrub	L, R, S	DaL, DaR, DaS
7	14/10/2019	Autumn	<i>Centella asiatica</i> (খানকুনা)	Near Rail Gate	Herb	L, R, S	ThL, ThR, ThS
8	14/10/2019	Autumn	<i>Catharanthus roseus</i> (নয়নতারা)	Central Mosque	Herb	L, R, S	NL, NR, NS
9	14/10/2019	Autumn	<i>Terminalia arjuna</i> (অর্জুন)	Alaol Hall	Tree	L, R, S	ArL, ArR, ArS
10	05/02/2020	Winter	<i>Mimosa pudica</i> (লজ্জাবতী)	Biol. Sci. Faculty	Herb	L, R, S	LL, LR, LF
11	05/02/2020	Winter	<i>Mikania micrantha</i> (জার্মানি লতা)	Biol. Sci. Faculty	Herb	L, R, S	GL, GR, GS
12	07/04/2021	Summer	<i>Terminalia chebula</i> (হরতিক)	Biol. Sci. Faculty	Tree	L, R, S	HL, HR, HS
13	10/04/2021	Summer	<i>Phyllanthus emblica</i> (আমলকী)	Biol. Sci. Faculty	Tree	L, R, S	AL, AR, AS
14	18/04/2021	Summer	<i>Mentha spicata</i> (পুদিনা)	Zero Point	Shrub	L, R, S	PL, PR, PS
15	23/04/2021	Summer	<i>Terminalia bellirica</i> (বহুড়া)	2 No. Gate	Tree	L, R, S	BoL, BoR, BoS
16	23/04/2021	Summer	<i>Azadirachta indica</i> (নিমি)	2 No. Gate	Tree	L, R, S	NeL, NeR, NeS

Note: Leaf: L; Root: R; Stem: S. Biological Sciences Faculty: Biol. Sci. Faculty.

<https://doi.org/10.1371/journal.pone.0269962.t002>

## Isolation of endophytic bacteria

The total procedure was performed according to Ferreira et al., 2008, where 48 collected plant parts (2–3 cm length) were cleaned under running tap water to remove debris and then air dried [37]. Surface sterilization was carried out by rinsing them with Tween-20 for 10 minutes, followed by further washing with dH<sub>2</sub>O at least 7 times. After that, samples were dipped into 70% alcohol for 30 seconds and then washed with dH<sub>2</sub>O. Twenty (20.0) ml of 0.2% Hg<sub>2</sub>Cl<sub>2</sub> solution was added to the samples in a beaker, which was placed on a shaker at 240 rpm for 5 minutes at 27°C. Then, the samples were washed again with dH<sub>2</sub>O at least 7 times. The final samples rinsed water was used as a control and spread onto nutrient agar plates [38], which contained (g/L)—peptone 5.00, beef extract 2.00, yeast extract 3.00, NaCl 5.00 and agar 18.00, where the pH was adjusted to 7.0. For the isolation of endophytic bacteria, samples were further treated in sterile phosphate-buffered saline (PBS) [39] containing (g/L) NaCl 8.00, KCl 0.20, Na<sub>2</sub>HPO<sub>4</sub> 1.44 and KH<sub>2</sub>PO<sub>4</sub> 0.24, where the pH was adjusted to 7.4 and maintained at 28°C under 50 rpm agitation. All plates, including the control, were incubated at 37°C for 5 days, and the number of CFUs was determined (Table 3) to estimate bacterial population density according to Addisu and Kiros, 2016 [38]. Following purification, morphologically distinct colonies were identified by observing colony characteristics such as gram nature, color, and shape using a binocular biological microscope (XSZ-107BN), where colonies of similar morphological features were grouped into the same species [40, 41]. Thus, isolates were selected, cultured, purified and stored in the laboratory at -80°C in glycerol stock (50%) solution for further studies.

## Phenotypic and biochemical characterization of endophytic bacterial isolates

Standard tests for morphological and biochemical analysis were performed for the identification of endophytic bacteria. They were characterized by Gram staining and biochemical tests as described in the Cowan and Steel's Manual for the identification of medical bacteria [42]. For the activities of oxidase, catalase, citrate utilization, indole production, methyl-red (MR),

**Table 3. List of isolated bacterial isolates and host medicinal plants.**

Serial No.	Sample Code	Host Medicinal Plant	Plant parts used
1	GL	<i>Mikania micrantha</i>	Leaf
2	GR		Root
3	LL1	<i>Mimosa pudica</i>	Leaf
4	LL2		Leaf
5	LF		Stem
6	HL1	<i>Terminalia chebula</i>	Leaf
7	HL2		Leaf
8	HS1		Stem
9	HS2		Stem
10	AL1	<i>Phyllanthus emblica</i>	Leaf
11	AL2		Leaf
12	AS1		Stem
13	AS2		Stem
14	PL1	<i>Mentha spicata</i>	Leaf
15	PL2		Leaf
16	PS1		Stem

<https://doi.org/10.1371/journal.pone.0269962.t003>

Voges-Proskauer (VP), urease production, and mannitol salt fermentation, isolates were biochemically analyzed [42]. Then, the standard protocol of Bergey's Manual of Systemic Bacteriology was followed for identification of isolates provisionally up to the species level [43].

### Determination of antibiotic sensitivity

The susceptibility of five finally identified isolates to different antibacterial agents was measured *in vitro* by employing the modified Kirby-Bauer method [44]. This method helps to determine the efficiency of a drug rapidly by measuring the diameter of the zone of inhibition that results from diffusion of the agent into the medium surrounding the disc [45]. Ten commercially available antibiotic discs (Himedia, India) were used for the tests (Table 4).

### Statistical analysis

Triplicate data were taken in all the cases during isolation, biochemical analysis and antibiotic sensitivity tests of the selected isolates. The results were analyzed according to the mean value  $\pm$  standard deviation (SD) in triplicate. Microsoft Excel Software, version 2010, was used to calculate means and standard deviations by capturing all relevant data.

### Molecular identification of bacteria

Genomic DNA was extracted [46] and stored at  $-20^{\circ}\text{C}$ . Following a standard protocol, the DNA concentration was measured by a Thermo Scientific NanoDrop 2000 spectrophotometer (Thermo Scientific, USA) following a standard protocol. Polymerase chain reaction (PCR) was carried out for the detection of bacteria using previously published primers and targeted genes [47, 48]. The Basic Local Alignment Search Tool (BLAST) was used to determine primer specificity by searching for similar sequences in the microbial genome. During all experiments, positive and negative controls were carried out. The total composition of the target gene, primer sequences, cycling parameters, PCR master mixture and amplicon size (bp) were determined for PCR amplifications in a thermal cycler (NyxTechnik) and are shown in Table 5.

Amplified PCR products were then analyzed by electrophoresis (Micro-Bio-Tech Brand) in 2% (w/v) agarose gel in 1 $\times$ TAE buffer, stained with ethidium bromide (1%) and compared with marker DNA (GeneRuler 1 kb DNA Ladder), finally visualized under ultraviolet (UV)

**Table 4. Antibiotic sensitivity test result.**

Serial No.	Name of Antibiotics	Disc Code	Disc Potency ( $\mu\text{g}$ )	Diameter of Inhibition (mm)				
				LL1	LL2	LF	GL	GR
1	Penicillin G	P	10	0 (R)	20 (R)	21(R)	13 (R)	20 (R)
2	Chloramphenicol	C	30	29 (S)	24 (S)	30 (S)	27 (S)	30 (S)
3	Ampicillin	AMP	25	12 (I)	25 (S)	23 (S)	20 (S)	24 (S)
4	Streptomycin	S	10	23 (S)	33 (S)	24 (S)	24 (S)	25 (S)
5	Vancomycin	VA	30	23 (S)	30 (S)	25 (S)	25 (S)	25 (S)
6	Norfloxacin	NX	10	25 (S)	21 (S)	30 (S)	30 (S)	32 (S)
7	Tetracycline	TE	30	22 (S)	12 (R)	24 (S)	20 (S)	22 (S)
8	Nalidixic Acid	NA	30	26 (S)	26 (S)	29 (S)	27 (S)	30 (S)
9	Erythromycin	E	15	27 (S)	13 (R)	28 (S)	25 (S)	29 (S)
10	Ceftriaxone	CTR	30	26 (S)	15 (R)	31 (S)	22 (S)	32 (S)

**Note:** R = Resistant, S = Sensitive, I = Intermediate

<https://doi.org/10.1371/journal.pone.0269962.t004>

**Table 5. Target genes, primer sequences, cyclic conditions, PCR master mixture composition and amplicon size.**

Target gene	Primer sequence (5'-3')	Cycling parameters	Total Composition of PCR master mixture	Amplicon size (bp)	Reference (s)
Common Bacterial 16S rDNA	8F-AGAGTTTGATCCTGGCTCAG 805R-GACTACCAGGGTATCTAAT	5 min at 95°C, 35 cycles of 95°C for 40 s, 57°C for 50 s and 72°C for 1 min	For 10 µl: 5 µl master mix, 2 µl template, 1 µl <sup>a</sup> and 1 µl <sup>b</sup> , 1 µl water	800	[47, 48]

a = forward primer; b = reverse primer; s = seconds

<https://doi.org/10.1371/journal.pone.0269962.t005>

trans-illuminator (Benda company) and then photographed. Then, PCR products were purified by an ATP<sup>TM</sup> Gel/PCR Fragment DNA Extraction Kit (Catalog No. ADF100/ADF300).

Five biochemically identified bacterial isolates were then sent for sequencing (Macrogen, South Korea). After sequencing, the results were visualized in DNA Baser software (V 5.15) and analyzed by the BLAST program in NCBI [49]. Then, the sequences were submitted to the GenBank database. Phylogenetic tree construction and evolutionary analyses were performed for every five isolates between BLAST searches of identified bacteria using MEGA 11 software [50]. The maximum composite likelihood method was used for computing evolutionary distances [51].

### Screening for growth-promoting parameters

**Indole acetic acid (IAA) production.** The IAA production potential was calculated as per Gordon and Weber [46]. The endophytic bacterial isolates were grown on ISP2 broth containing 0.2% L-tryptophan incubated at 37°C with shaking at 150 rpm for 5 days. Cultures were centrifuged at 12,000 rpm for 10 min. Development of a pink-red color confirms IAA production by the addition of 0.5% Salkowski reagent into 1 ml of cell free supernatant. Estimation of IAA was measured by taking the absorbance at 530 nm using a spectrophotometer, and the amount of IAA was calculated in µg/ml compared with the standard curve of IAA.

**Ammonia production.** Ammonia production was estimated using the modified qualitative method [6], where endophytic isolates were incubated in peptone water broth at 37°C at 150 rpm for 7 to 14 days. Then, 0.5 ml of Nessler's reagent was added to water broth, and the development of a brown to yellow color confirmed ammonia production. The absorbance was measured at 530 nm using a spectrophotometer, and ammonia production was expressed in mg/ml when compared with the standard curve of (NH<sub>4</sub>)<sub>2</sub>SO<sub>4</sub>.

**Production of hydrolytic enzymes.** The proteolytic activity of endophytic bacteria was determined by streaking the isolates on skim milk agar medium. The isolates were single-streaked in skim milk agar medium and incubated at 37°C for 24–48 hours. A clear hollow zone around the areas where the organism has grown indicates proteolytic activity.

**Preparation of crude extract.** Isolated endophytic bacterial crude extracts were prepared following the methods described by Deljou and Goudarzi, 2016 with some modifications [52]. Endophytic bacterial isolates were inoculated in a 125 mL Erlenmeyer flask containing 25 mL nutrient broth. A rotary incubator shaker was used for incubation at 150 rpm and 37°C for 24 hours and 48 hours. After incubation, centrifugation was performed at 12,000 rpm for 10 minutes, and the cell and supernatant were extracted with organic solvent (1:1 v/v) using ethyl acetate (EA). A rotary vacuum evaporator was used to retrieve crude extracts by evaporating the organic solvents. The dry weight of the crude extracts was measured using a digital weighing machine and dissolved in 1% dimethyl sulfoxide (DMSO).

### Determination of antioxidant compounds

**Total phenolic content (TPC).** The total phenolic content was measured by following Folin-Ciocalteu's colorimetric method [53], where 0.1 mL of sample and 0.5 mL of Folin-

Ciocalteu were mixed with 6.0 mL of double-distilled water. After 1 min, 1.5 mL of 20% Na<sub>2</sub>CO<sub>3</sub> (Merck, Germany) was added, and the total volume was made up to 10.0 mL with double-distilled water. The mixture was incubated for 2 h at 25°C. The absorbance was measured at 760 nm using a spectrophotometer against the blank solution containing all the reagents and the appropriate volume of the same solvent used for the sample. Gallic acid was used as the control indicator containing all the reaction agents except the sample.

**Total flavonoid content (TFC).** The total flavonoid content was measured by using the AlCl<sub>3</sub> colorimetric method [54] with slight modifications. Quercetin was used to make the calibration curve. One milligram of quercetin was dissolved in methanol and then diluted to 20, 40, 60, 80, and 100 µg/mL. Then, 0.5 mL diluted standard solutions were separately mixed with 1.5 mL of methanol, 0.1 mL of 10% AlCl<sub>3</sub>, 0.1 mL of 1 M potassium acetate, and 2.8 mL of distilled water. After incubation at room temperature for 30 min, the absorbance of the reaction mixture was measured at 415 nm using a UV-Vis spectrophotometer. The amount of 10% AlCl<sub>3</sub> was substituted by the same amount of distilled water in the blank. Similarly, 0.5 mL of sample solution was used with AlCl<sub>3</sub> for determination of flavonoid content as described above.

### ***In silico* analysis of bioactive secondary metabolite genes and compounds**

**Detection of bioactive secondary metabolite regions.** The antiSMASH (antibiotics and Secondary Metabolite Analysis Shell) webserver tool (bacterial version) was used to detect the secondary metabolite regions of the isolated endophytes. First, the whole genome sequences and accession numbers of the bacterial strains were obtained from NCBI, and then sequences were uploaded as data input. KnownClusterBlast, SubClusterBlast, and ActiveSiteFinder were marked as featured options. From the graphical output, secondary metabolite regions and their types were identified.

**Prediction of bioactive secondary compounds.** The antiSMASH ([antismash.secondarymetabolites.org](https://antismash.secondarymetabolites.org)) and Minimal Information about a Biosynthetic Gene cluster-MIBiG ([mibig.secondarymetabolites.org](https://mibig.secondarymetabolites.org)) databases were used to identify the proximate secondary metabolite regions. According to the cluster, different compounds were found as hits through Knowledge Blast.

**Analysis of biosynthetic genes and interaction of proteins.** Secondary metabolite gene clusters were searched for core and additional biosynthetic genes involved in metabolite production. Later, the STRING database ([string-db.org](https://string-db.org)) was used to identify and analyze the protein-protein interaction between the core genes involved in secondary metabolism.

**Analysis of PKS/NRPS domains.** Statistical preferences of putative polyketide synthase (PKS) and nonribosomal peptide synthetase (NRPS) domains at the genus level were analyzed via the SBSPKS v2 web server tool ([www.nii.ac.in/~pkscdb/sbspks](http://www.nii.ac.in/~pkscdb/sbspks)) [55]. Datasets were generated from the MIBiG repository.

**Molecular detection of biosynthetic genes.** Four sets of degenerate primers were designed according to the study Ayuso-Sacido and Genilloud, 2005 [56], targeting the universal bacterial PKS (polyketide synthase) and NRPS (nonribosomal peptide synthetase) genes along with chalcone synthase (CHS) and ACC deaminase (acdS) gene primers.

PCR conditions were as follows: initial denaturation at 95°C for 4 min, followed by 30 cycles of denaturation at 94°C for 1 min, annealing at 57°C for NRPS, 58°C for PKS, 52°C for CHS and 55°C for ACCD primers for 1 min and extension at 72°C for 1 min with a final extension step at 72°C for 4 min.

**Molecular docking of bioactive compounds against the SARS-COV2 protein.** The crystal structures of coronavirus 3CL<sup>PFO</sup> used in the docking analysis were retrieved from the

Protein Databank (<http://www.rcsb.org>) with its PDB identification code (6lu7) [57, 58]. The 3CL<sup>pro</sup> structures were processed by eliminating existing ligands and water molecules, while missing hydrogen atoms were added according to the amino acid protonation state at pH 7.0 employing the Autodock version 4.2 program (Scripps Research Institute, La Jolla, CA) [59].

The structure data format (SDF) structures of the 3CL<sup>pro</sup> reference inhibitor lopinavir and the identified endophytic bioactive compounds were retrieved from the PubChem database ([www.pubchem.ncbi.nlm.nih.gov](http://www.pubchem.ncbi.nlm.nih.gov)) [60].

Virtual screening of the coronavirus 3CL<sup>pro</sup> active regions and determination of the binding affinities of the compounds and reference inhibitor were carried out using AutoDockvina 4.2 with full ligand flexibility. The molecular interactions between proteins and respective ligands with higher binding affinity were viewed using Discovery Studio Visualizer version 16.

**ADMET and drug-likeness prediction.** After the molecular docking studies, the absorption, distribution, metabolism, elimination and toxicity (ADMET) of the docked metabolites were screened using the online tools admetSAR ([lmmd.ecust.edu.cn](http://lmmd.ecust.edu.cn)) [61] and SwissADME ([www.Swissadme.ch](http://www.Swissadme.ch)) to predict their important pharmacokinetic properties [62].

**<sup>1</sup>H-NMR spectrophotometry.** The bacterial crude extract was sent to INARS Laboratory, Bangladesh Council of Scientific and Industrial Research (BCSIR), DHAKA for <sup>1</sup>HNMR analysis. At BCSIR, data were acquired on a 400 MHz spectrometer (Bruker Corporation).

## Results

### Isolation of endophytic bacteria

Forty-eight plant parts (3 parts from 16 plants each) were subjected to surface sterilization [63], triturated with autoclaved phosphate-buffered saline (PBS) [64, 65], and then used to isolate endophytic bacteria. After spreading the plant extracts derived from forty-eight (48) plant parts over solid nutrient agar (NA) media, several bacterial colonies were found, and sixteen pure colonies were selected (Table 3) after incubation for 48 hours at 37°C. Then, several sub-cultures were performed to isolate pure cultures from different types of endophytic bacteria (Fig 1) and finally preserved in a 4°C refrigerator for further studies.

**Identification of endophytic bacteria by biochemical characterization.** Pure cultures of five selected types of isolates were then subjected to a series of biochemical tests (Table 6) as described in Bergey's Manual for Determinative Bacteriology [66]. After the Gram staining procedure, four isolates, LL1, LL2, LF, and GL, showed violet colors, whereas GR showed pink colors under a microscope. Thus, GR was considered gram-negative, and the others were considered gram-positive bacteria. LL1, LF, and GR were rod in shape under a microscope, while LL2 and GL were identified as coccus-shaped bacteria. In the catalase test, four samples, LL1, LL2, LF, and GL, produced bubbles after the addition of H<sub>2</sub>O<sub>2</sub>, which indicated the presence of the catalase enzyme. Sample GR failed to produce any bubbles and thus was catalase-negative. In the oxidase test, all five isolates, LL1, LL2, LF, GL, and GR, showed a deep blue color within 10 seconds, indicating the ability to produce oxidase enzymes as a positive result. In the indole production test, the appearance of a red ring indicates a positive result. All five isolates tested negative, as no red ring appeared, indicating the absence of tryptophanase enzyme. Four isolates, LL1, LL2, LF, and GL, exhibited red color formation, indicating the capacity to produce and maintain a stable acid end product. Sample GR, on the other hand, was unable to show red color formation and thus tested negative. In the Voges-Proskauer test, all five samples were unable to yield red color formation, which indicated that they were unable to produce butylene glycol. Thus, all the samples were tested negative. In the citrate utilization test, only isolate LL2 was found to produce a blue color as a positive result, which indicated that the other four isolates were unable to utilize citrate due to the absence of citrate-utilizing enzymes.

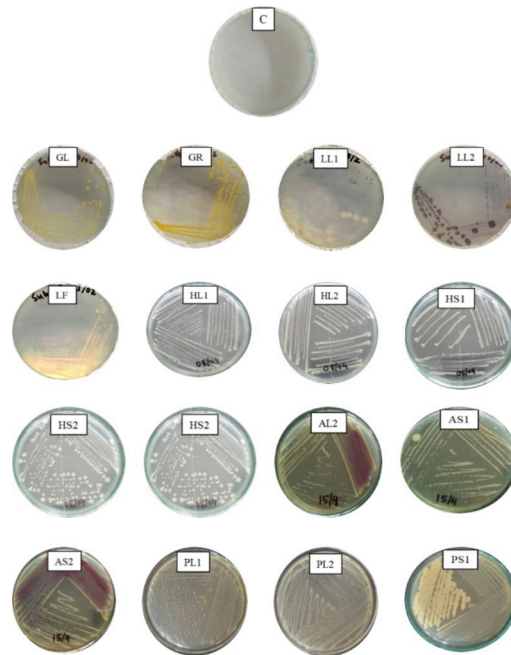


**Fig 1. Pure cultures of sixteen isolated endophytic bacteria labeled as their sample codes (GL, GR, LL1, LL2 LF, HL1, HL2, HS1, HS2, AL1, AL2, AS1, AS2, PL1, PL2, PS1); Control (C) indicates no growth of bacteria in the medium.**

<https://doi.org/10.1371/journal.pone.0269962.g001>

Mannitol salt agar (MSA) media was used to identify the isolates growing on high salt concentrations, and a positive test consisted of a color change from red to yellow, indicating a pH change to acidic. Among the five isolates, only LL1 showed a positive result (Table 6).

**Antibiotic sensitivity test.** Ten types of antibiotic discs (Himedia, India) were used to test the sensitivity [44], where every isolate showed resistance toward penicillin G. In addition, isolate LL2 showed resistance (R) to tetracycline, erythromycin and ceftriaxone. LL1 expressed

**Table 6. Summary of morphological and biochemical characterization.**

Morphological and Biochemical Characteristics	ISOLATE CODE				
	LL1	LL2	LF	GL	GR
<b>Morphological Characteristics</b>					
Colony Color	Yellowish	Purple	White	Yellowish	Yellow
Gram Staining	+	+	+	+	-
Shape	Rod	Cocci	Rod	Cocci	Rod
<b>Biochemical tests</b>					
Catalase	+	+	+	+	-
Oxidase	+	+	+	+	+
Indole	-	-	-	-	-
Methyl Red	+	+	+	+	-
VP	-	-	-	-	-
Mannitol Salt Fermentation	-	+	-	-	-
Citrate Utilization	+	-	-	-	-
<b>Identified Strain</b> (provisionally)	<i>Bacillus spp.</i>	<i>Staphylococcus spp.</i>	<i>Bacillus spp.</i>	<i>Staphylococcus intermedius</i>	<i>Pseudomonas spp.</i>

Note: (+) indicates a positive result and (-) indicates a negative result.

<https://doi.org/10.1371/journal.pone.0269962.t006>

intermediate (I) sensitivity to ampicillin [67], and the rest of the isolates were found to be sensitive to all antibiotics (Table 4).

**Identification of bacteria depends on morphological and biochemical analysis.** The overall morphological and biochemical test results of five distinct isolates and their identifications [66] are listed in Table 6.

**Identification of bacterial strains by molecular characterization.** After extraction of genomic DNA from five isolates, DNA concentration and purity were measured by a Nano-drop 2000 (Thermo Scientific, USA). Extracted DNA of five bacterial isolates was then amplified by 16S rDNA primers. Gel electrophoresis was performed afterwards on a 2% agarose gel and stained with ethidium bromide. After that, the gel was visualized by a UV transilluminator (Benda Company) (Fig 2). After PCR amplification of five bacterial isolates, they were sent for Sanger sequencing by Macrogen's sequencing service (South Korea). Purified PCR products along with their respective primers were sequenced and finally confirmed up to their species. Isolates LL1, LL2, LF, GL and GR were thus identified as *Priestia megaterium*, *Staphylococcus caprae*, *Neobacillus drentensis*, *Micrococcus yunnanensis*, and *Sphingomonas paucimobiliz*, respectively, with 99% identity with an e value of 0 in NCBI BLAST (Basic Local Alignment Search Tool) analysis. After analysis by the BLAST program, isolate information was submitted to GenBank by using the GenBank submission portal. Then, the accession numbers for the nucleotide sequences were obtained as MW494406, MW494408, MW494401, MW494402, and MZ021340.

The five isolates were then subjected to phylogenetic tree construction according to their 16S rRNA sequences with MEGA 11 Version 5.0 Software (Fig 3). The neighbor-joining method was used to interpret evolutionary history. The optimal tree is demonstrated with the sum of branch length = 0.06596246. The scale is shown in the tree, with branch lengths in the same units as those of the evolutionary distances used to infer the phylogenetic tree. The evolutionary distances were enumerated by applying the maximum composite likelihood method [51] in units of the number of base substitutions per site. The analysis has 20 nucleotide sequences. Codon positions comprised with 1st+2nd+3rd+Noncoding. All cryptic positions were eliminated for each sequence pair. There were a total of 1349 positions in the final dataset. Evolutionary analyses were conducted in MEGA 11 [50].

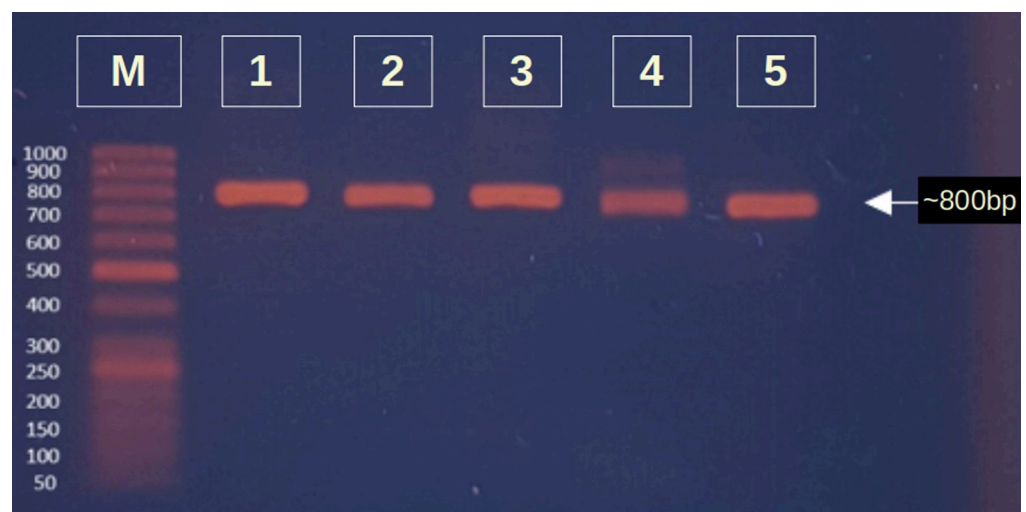


**Fig 2. Electrophoretic separation (2% agarose) of the 16S rDNA gene of different isolates.** M: 50 bp DNA ladder; 1: LL1; 2: LL2; 3: LF; 4: GL; 5: GR.

<https://doi.org/10.1371/journal.pone.0269962.g002>

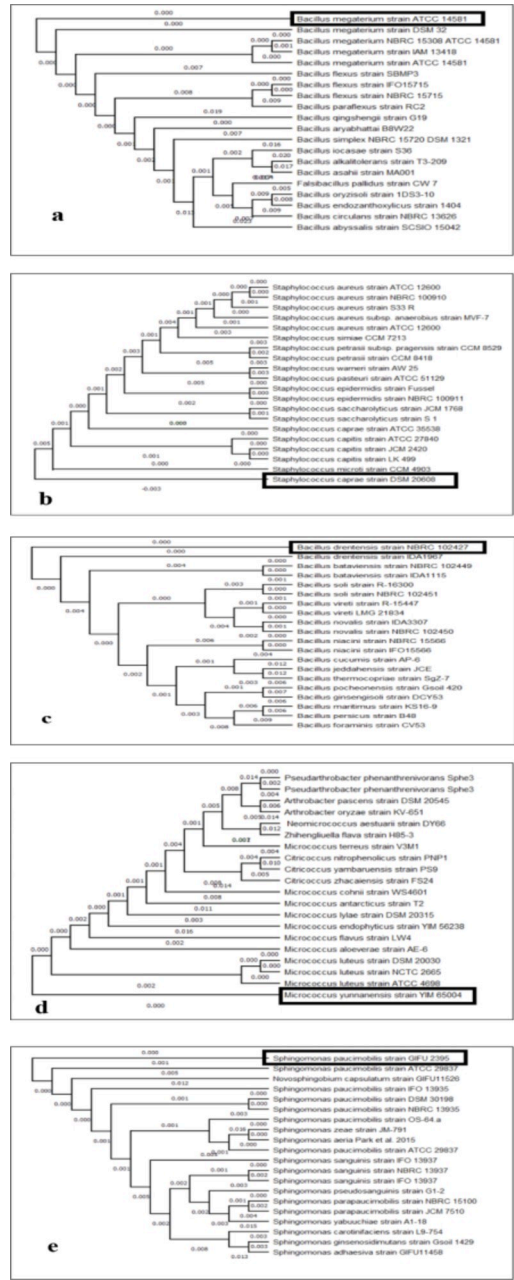


**Fig 3. Phylogenetic tree of isolates.** (a) *Priestia megaterium*, (b) *Staphylococcus caprae*, (c) *Bacillus drementensis*, (d) *Micrococcus yunnanensis*, (e) *Sphingomonas paucimobilis*.

<https://doi.org/10.1371/journal.pone.0269962.g003>

**Screening for growth-promoting parameters of isolated bacteria.** Quantitative estimation of all isolates was performed in ISP2 broth medium [68], and the indole acetic acid (IAA) production rate ranged from 14.26 to 25.56 µg/mL (Table 7). A maximum IAA yield of 25.561 ± 0.05 µg/mL was observed by isolate GR (*Sphingomonas paucimobilis*). IAA solution was used as a standard, and the concentration of samples was estimated by the standard curve (Fig 4).

Quantitative estimation of ammonia production by all isolates in peptone water broth ranging from 5.3 to 24.98 mg/mL. Isolate LL2 (*Staphylococcus caprae*) produced the maximum

Table 7. Estimation of IAA, ammonia, TPC and TFC by five isolates.

Name of isolates	IAA		Ammonia		TPC		TFC	
	Absorbance (530 nm)	Concentration (µg/mL)	Absorbance (530 nm)	Concentration (µg/mL)	Absorbance (760 nm)	Concentration (µg/mL)	Absorbance (415 nm)	Concentration (µg/mL)
<i>Priestia megaterium</i> (LL1)	0.416	14.268 ± 0.05	1.074	20.23 ± 0.01	0.327	258.901 ± 0.02	0.2237	36.09 ± 0.02
<i>Staphylococcus caprae</i> (LL2)	0.727	*23.902 ± 0.06	1.211	**24.98 ± 0.03	0.467	**406.653 ± 0.01	0.2971	**45.18 ± 0.06
<i>Neobacillus drentensis</i> (LF)	0.646	*23.612 ± 0.01	0.662	5.98 ± 0.01	0.366	300.060 ± 0.01	0.2381	38.92 ± 0.05
<i>Micrococcus yunnanensis</i> (GL)	0.536	19.143 ± 0.20	0.615	4.35 ± 0.02	0.314	245.181 ± 0.05	0.1380	19.29 ± 0.01
<i>Sphingomonas paucimobiliz</i> (GR)	0.694	**25.561 ± 0.05	0.644	5.32 ± 0.04	0.302	232.517 ± 0.05	0.1416	20.01 ± 0.02

Note: \*\* indicates maximum result

<https://doi.org/10.1371/journal.pone.0269962.t007>

amount of ammonia (24.98±0.03 mg/mL) (Table 7). Ammonium sulfate was used as the standard, and the concentration of samples was estimated by the standard curve (Fig 4).

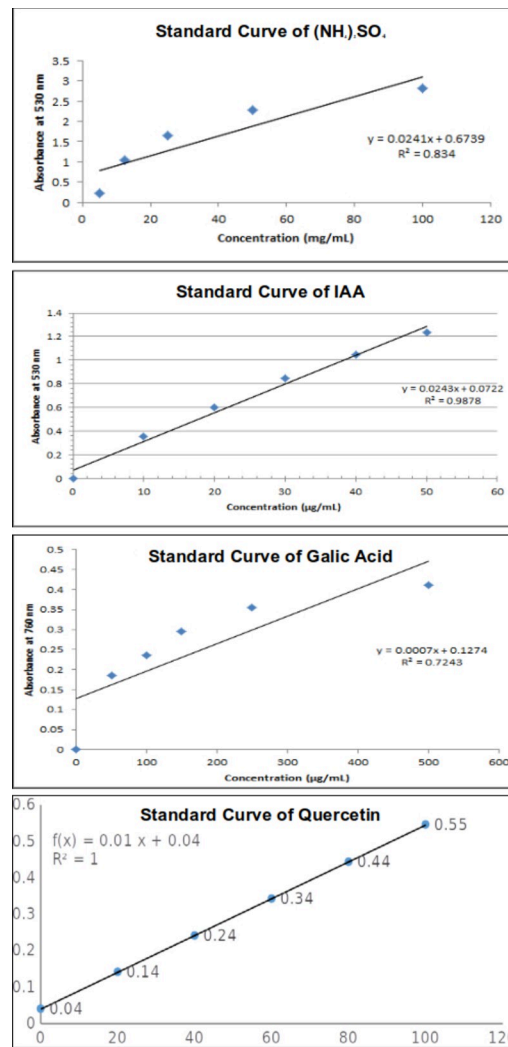


Fig 4. Standard curves of ammonium sulfate, indole acetic acid, gallic acid and quercetin.

<https://doi.org/10.1371/journal.pone.0269962.g004>

Out of five isolates, two isolates were found to be positive for protease enzyme activity. *Priestia megaterium* (LL1) and *Staphylococcus caprae* (LL2) isolates showed clear degradation of the protein (Fig 5) in skim milk agar [69].

**Determination of antioxidant compounds from crude extracts.** Crude extracts (extra-cellular secondary metabolites) of isolated endophytic bacteria were estimated by using ethyl acetate solvent, and each sample was incubated for 24 hours and 48 hours [52]. *Staphylococcus caprae* (LL2) showed the maximum result, while *Sphingomonas paucimobiliz* (GR) showed the minimum (Table 8). Ethyl acetate (EA) extracts were stored in 1% dimethyl sulfoxide (DMSO) for further antioxidant and metabolite analysis [70].

Ethyl acetate extracts of the isolated bacteria were processed to analyze total phenolic compounds [71]. Isolate LL2 exhibited the maximum result ( $406.653 \pm 0.01 \mu\text{g/mL}$ ), and isolate GR exhibited the lowest ( $232.517 \pm 0.05 \mu\text{g/mL}$ ) (Table 7). Gallic acid was used as the standard to estimate the TPC (Fig 4).

Ethyl acetate extracts of the isolated bacteria were processed to analyze total flavonoid compounds. Isolate *Staphylococcus caprae* (LL2) exhibited the maximum result ( $45.18 \pm 0.06 \mu\text{g/mL}$ ), and isolate *Micrococcus yunnanensis* (GL) exhibited the lowest result ( $19.29 \pm 0.01 \mu\text{g/mL}$ ) (Table 7). Quercetin was used as the standard [70] to estimate the TPC (Fig 4).

**In silico analysis of bioactive secondary metabolite genes and compounds.** Antibiotics and secondary metabolite analysis shell (antiSMASH) server was used to identify different secondary metabolite regions present in the genome of identified bacterial strains (Fig 6). The whole-genome sequences were taken from NCBI and input to the antiSMASH server. A total of 13 different bioactive secondary metabolite regions were identified within five isolates. Terpene was the most common type of cluster found in each isolate, followed by Type III polyketide synthase (T3PKS) and the siderophore cluster. *Priestia megaterium* had the highest number (9) of bioactive regions among the isolates (Fig 7).

After the identification of core biosynthetic gene clusters by antiSMASH, the MIBig (Minimal Information about a Biosynthetic Gene cluster) specification was used to predict the bioactive compounds according to the region and their type (Table 9). Nine (9) putative compounds were found from the whole genome sequences of identified endophytes. The most similar known cluster was searched for the identified query clusters, and based on a percentage

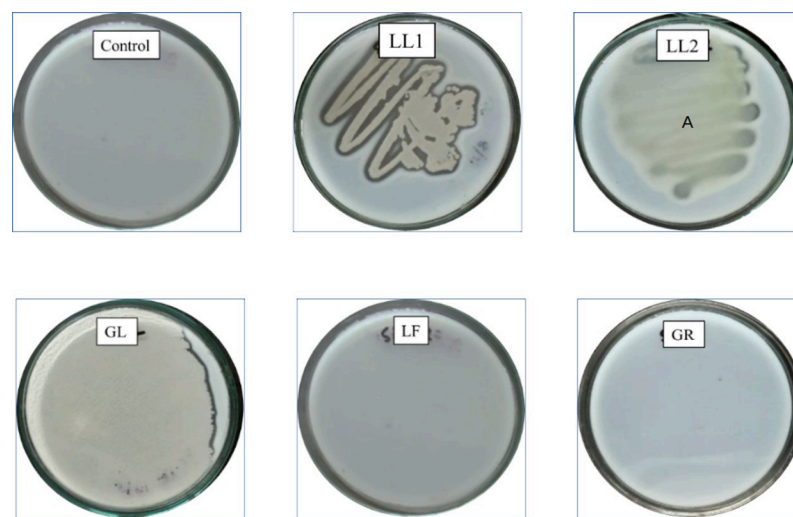


**Fig 5. Isolates in skim milk agar.** LL1 (*Priestia megaterium*) and LL2 (*Staphylococcus caprae*) represented protease enzyme activity with a clear hollow degradation of protein throughout the inoculation area.

<https://doi.org/10.1371/journal.pone.0269962.g005>

**Table 8. Production of crude extracts from isolated endophytic bacteria.**

Name of isolates	Incubation Period (hour)	Quantity of Crude Extract (gm)
<i>Priestia megaterium</i> (LL1)	24	0.34 ± 0.02
	48	0.36 ± 0.03
<i>Staphylococcus caprae</i> (LL2)	24	**0.45 ± 0.01
	48	**0.48 ± 0.01
<i>Neobacillus drentensis</i> (LF)	24	0.16 ± 0.02
	48	0.22 ± 0.03
<i>Micrococcus yunnanensis</i> (GL)	24	0.14 ± 0.04
	48	0.21 ± 0.01
<i>Sphingomonas paucimobiliz</i> (GR)	24	0.12 ± 0.05
	48	0.17 ± 0.04

**Note:** \*\* indicates maximum results

<https://doi.org/10.1371/journal.pone.0269962.t008>

similarity, their molecular compounds were predicted as hits (Fig 8). MIBiG produced the output file with details of biosynthetic genes (core and additional), transport-related genes, regulatory genes and other genes. Compound structures were also obtained from the output (Fig 8). Predicted similar compounds (Table 9) were analyzed through their core and additional biosynthetic genes obtained from the antiSMASH and MIBiG datasets (Table 10). The interaction of those genes and their protein products was checked through the STRING database (version 11.0) [72]. All genes associated with those 9 gene clusters of identified compounds were programmed to be enlisted according to the query in the Uniprot database of protein. The highest 12 biosynthetic genes were identified in the gene cluster responsible for the fengycin compound and likely 9 genes for surfactin, 6 genes for bacitracin, 3 genes for zeaxanthin, and 4 genes for both the carotenoid and staphyloferrin A compounds (Table 9). All the genes were retrieved with enough protein data from the Uniprot server [73], but unfortunately, no genes could be retrieved for aureusmin, stenothrin, or microanamycin. As we have used the STRING server to expose the interaction between the genes and the proteins, these three compounds may be unable to produce any associated network. Interactions between genes involved in secondary

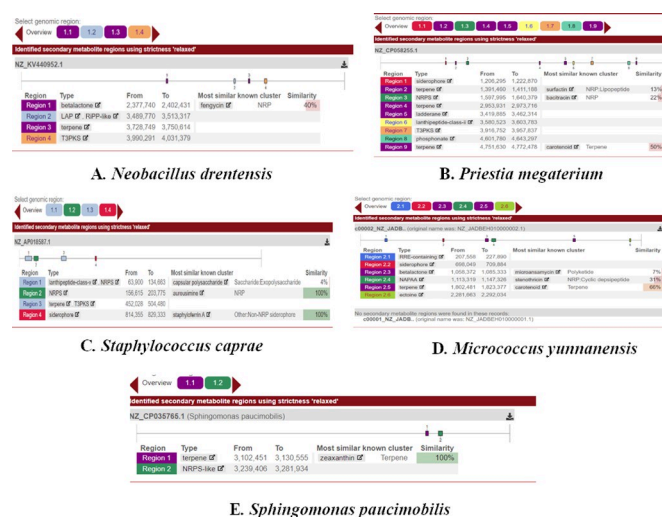


**Fig 6. Identification of secondary metabolite regions using the antiSMASH server.**

<https://doi.org/10.1371/journal.pone.0269962.g006>

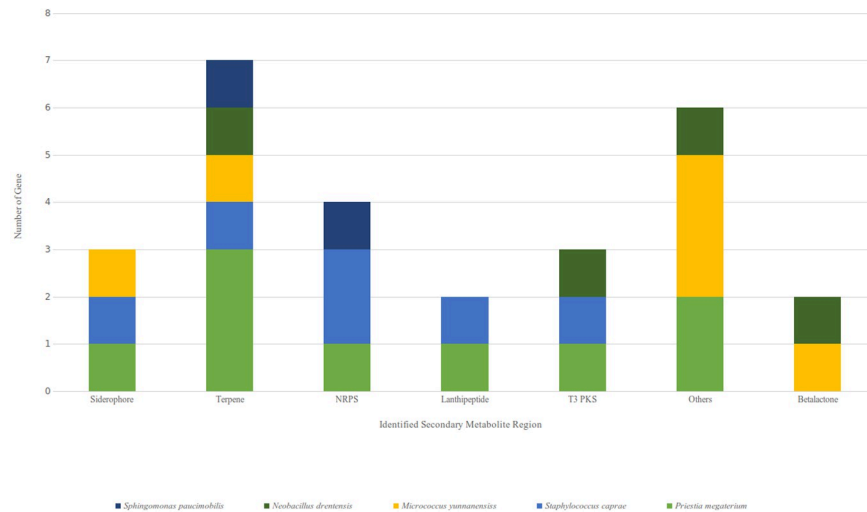


**Fig 7. Distribution of genes in identified biosynthetic gene clusters: NRPS Non ribosomal peptide synthetase, T3PKS = Type 3 polyketide synthase.**

<https://doi.org/10.1371/journal.pone.0269962.g007>

metabolite gene clusters of the compounds are shown in nodes and edges (Fig 9), where significant protein–protein interactions were observed according to the functional properties of the genes and their respective products. ClusterBlast results (from the MIBiG database) were further analyzed to measure the PKS (polyketide synthase) and NRPS (nonribosomal peptide synthetase) in a comparative source of endophytic bacteria at their sequenced species level [19]. SBSPKS v2 was used to carry out functional analyses of the PKS and NRPS domains (Fig 10). *Bacillus* was found to be rich in these domains, having confirmed and some hypothetical regions. A moderate percentage was found for *Staphylococcus* spp. possessing similar amounts and thus exhibited diverse types of PKSs and NRPSs. These particular conserved clusters are spotted domains of Fimicutes, Proteobacteria and Actinobacteria phyla [15].

The presence of biosynthetic genes was determined in the identified strains with four sets of gene-specific primers. PCR amplification of polyketide synthase (PKS), nonribosomal peptide synthetase (NRPS) [56], 1-aminocyclopropane-1-carboxylate deaminase (ACCD) [4], and chalcone synthase (CHS) [19] genes was performed for our identified strains. All strains showed a prominent band (amplicon size ~600–700 bp) for the NRPS gene [83] (Fig 11B). PKS candidate amplicons (~700–800 bp) were detected in *Priestia megaterium* (LL1), *Staphylococcus caprae* (LL2), *Micrococcus yunnanensis* (GL), and *Spingomonas paucimobiliz* (GR)

**Table 9. List of predicted bioactive compounds from gene clusters.** \*\* All the structures of the compound are given in the (S1 Fig).

Identified isolates	Compound	Type	Bioactivity
<i>Priestia megaterium</i> (LL1)	Surfactin	Nonribosomal peptide (NRP)-lipopeptide	Surfactant, Antibacterial Antiviral [74]
	Bacitracin	Nonribosomal peptide (NRP)	Broad-spectrum antibiotic [75]
	Carotenoid	Terpene	Antioxidant, a precursor of vitamin [76]
<i>Micrococcus yunnanensis</i> (GL)	Microansamycin	NRP- Cyclic depsipeptide	Antioxidant [77]
	Stenothricin	Terpene (nonalpha poly-amino acids like e-Polylysin)	Antibiotic [78]
<i>Staphylococcus caprae</i> (LL2)	Aureusimine	Nonribosomal peptide (NRP)	Potent antibiotic [79]
	Staphyloferrin A	Siderophore	Potent antibiotic [80]
<i>Neobacillus drentensis</i> (LF)	Fengycin	Betalactone	Antifungal [81]
<i>Spingomonas paucimobiliz</i> (GR)	Zeaxanthin	Terpene	Antioxidant [82]

<https://doi.org/10.1371/journal.pone.0269962.t009>

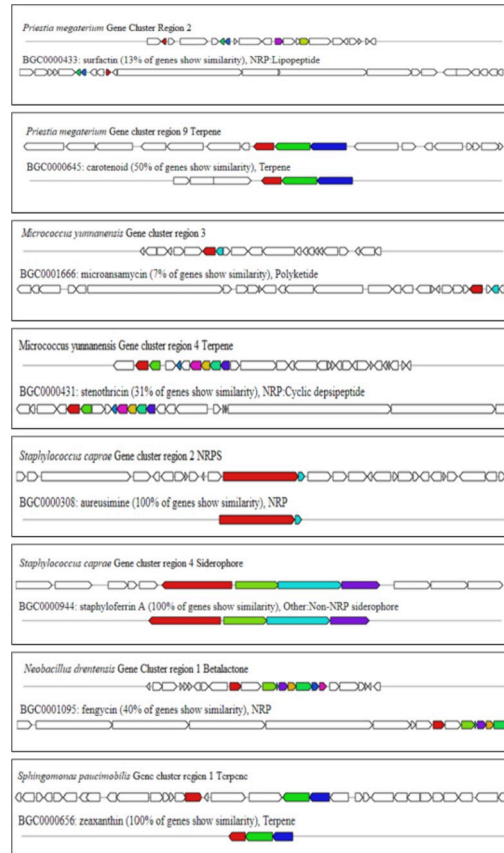


**Fig 8. Graphical representations of most similar known clusters as an output of ClusterBlast specified by the MIBiG repository.** Color codes represent similar gene regions.

<https://doi.org/10.1371/journal.pone.0269962.g008>

(Fig 11A). For the ACCD gene, only *Sphingomonas paucimobilis* (GR) was positive (Fig 11C), and all isolates showed negative results for the CHS gene, as no DNA band was found in PCR amplification (Fig 11D).

The binding energy from the docking analysis of bioactive compounds (5) and reference compound to 3-chymotrypsin-like protease (3CL<sup>Pro</sup>) of the novel SARS-COV-2 is represented in Table 11. The ligand–protein binding interactions according to the residues of our compound and macromolecule (3CL<sup>Pro</sup>) are shown in Fig 12A–12F. Protein–ligand interactions were exhibited through residues and bonds via 2D representation in Fig 13.

The results generated from the Lipinski and ADME/tox filtering analyses are presented in Table 12. Two compounds were found to be **required** for Lipinski analysis of the rule of five with corresponding favorable predicted ADME/tox parameters. The predicted physiochemical properties for the bioavailability of the lead compounds are further represented in Fig 14.

**<sup>1</sup>H-NMR metabolomics analysis.** With respect to the <sup>1</sup>H-NMR metabolite data, the proton number was calculated for each metabolite and we have found three metabolites: microansamycin (Fig 15A), aureusimine (Fig 15B) and surfactin (Fig 15C) in our bacterial sample.

## Discussion

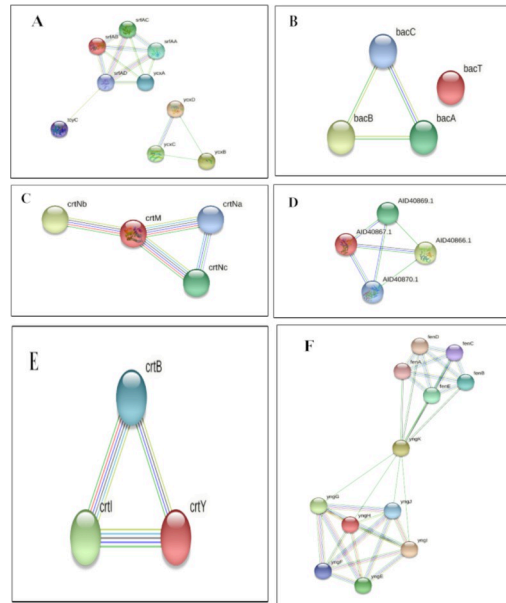
Plants possess thousands of microbes residing inside their various tissues and forming a mutual relationship. Every living plant on earth is host to one or more endophytes: bacteria or fungi that colonize living plant tissues by producing a wide variety of specialized metabolites

Table 10. List of responsible genes and proteins from the secondary metabolite gene clusters of the identified compounds.

Compound	Gene	Protein	Biological Process	Pathway
Surfactin	srfAA	Surfactin synthase subunit 1	<a href="#">Antibiotic biosynthetic process</a>	Surfactin biosynthesis
	srfAB	Surfactin synthase subunit 2		
	srfAC	Surfactin synthase subunit 3		
	srfAD	Surfactin synthase thioesterase subunit	Transport	Transmembrane transport
	ycxA	MFS type Transporter	Transport	Transmembrane transport
	ycxB	Uncategorized protein		
	ycxC	Transporter Protein	Transport	Transmembrane transport
	ycxD	Transcriptional regulator protein	DNA binding cofactor	Alpha amino acid metabolic pathway
	tcyC	L-cystine import ATP-binding protein	<a href="#">ATPase-coupled amino acid transmembrane transporter activity</a>	Amino acid transport pathway
Bacitracin	bacA	Prephenate decarboxylase	<a href="#">Antibiotic biosynthetic process</a>	Bacilysin biosynthesis
	bacB	H2HPP isomerase		
	bacC	bacilysin synthetase C		
	bacI	Thioesterase family protein		
	bacR	Transcriptional regulatory Protein	DNA binding	
	bacS	Histidine kinase	Regulation process	
Carotenoid	crtNa	CrtNa protein	<a href="#">Oxidoreductase activity</a>	Carotenoid biosynthesis
	crtNc	CrtNc protein	<a href="#">oxidoreductase activity</a>	
	crtM	4,4'-diapophytoene synthase	Transferase activity	
	crtNb	CrtNb protein	<a href="#">Oxidoreductase activity</a>	
Staphyloferrin A	sfaC (SAOUHSC_02433)	Staphyloferrin A synthetase	Nonribosomal peptide biosynthesis	Staphyloferrin biosynthesis
	sfaB (SAOUHSC_02434)	Staphyloferrin A synthetase	Nonribosomal peptide biosynthesis	
	sfaA (SAOUHSC_02435)	Staphyloferrin A Transporter	Siderophore transporter	
	iucC_3 (SAOUHSC_02436)	L-ornithine Racemase	Siderophore biosynthesis	Precursor biosynthesis
Zeaxanthine	crtY	Lycopene cyclase	<a href="#">lycopene beta cyclase activity</a>	<a href="#">carotenoid biosynthetic process</a>
	crtI	Phytoene dehydrogenase	<a href="#">oxidoreductase activity</a>	<a href="#">carotenoid biosynthetic process</a>
	crtB	Phytoene synthase	<a href="#">squalene synthase activity</a>	
Fengycin	yngE	Acyl-CoA carboxylase subunit beta	<a href="#">ligase activity</a>	
	yngF	Enoyl-CoA hydratase	<a href="#">catalytic activity</a>	
	yngG	Hydroxymethylglutaryl-CoA lyase	<a href="#">oxo-acid-lyase activity</a>	
	yngH	Acetyl-CoA carboxylase biotin carboxylase subunit	<a href="#">ATP binding</a>	
	yngI	AMP-binding protein	AMP-binding	
	yngJ	Acyl-CoA dehydrogenase	<a href="#">Oxidoreductase</a>	
	yngK	Glycoside hydrolase family protein	<a href="#">hydrolase activity</a>	
	fenA	fengycin synthetase A	Nonribosomal peptide synthetase	<a href="#">Antibiotic biosynthetic process</a>
	fenB	fengycin synthetase B		
	fenC	fengycin synthetase C		
fenD	fengycin synthetase D			
fenE	fengycin synthetase E			

<https://doi.org/10.1371/journal.pone.0269962.t010>

without causing any harm or disease to the host plants [29]. However, in the case of medicinal plants, relatively few endophytes have been studied thus far, and of course, for the endemic



**Fig 9. Predicted association of proteins of biosynthetic genes demonstrated by the STRING server.** (A) Surfactin, (B) bacitracin, (C) carotenoid, (D) staphyloferrin A, (E) zeaxanthin and (F) fengycin protein network. Line Indicator: Red Line–Presence of fusion evidence, Green Line- neighborhood evidence, Blue Line- cooccurrence evidence, Purple Line- experimental evidence, Yellow Line- textmining evidence, Light Blue Line- database evidence, Black Line- coexpression evidence.

<https://doi.org/10.1371/journal.pone.0269962.g009>

medicinal plants of Bangladesh as well. Therefore, one of the major objectives of this study is to isolate and characterize endophytic bacteria from our local medicinal plants to study their secondary metabolites, which have a wide range of applications in the global health sector.

Studies have revealed the capacity of endophytes to produce a diverse range of secondary metabolites [13]. Different types of important natural products, including antibiotics, antifungal, insecticidal, anticancer, immunosuppressant, antiviral, and volatile organic compounds, have been derived or synthesized from various endophytic bacteria. There has been growing

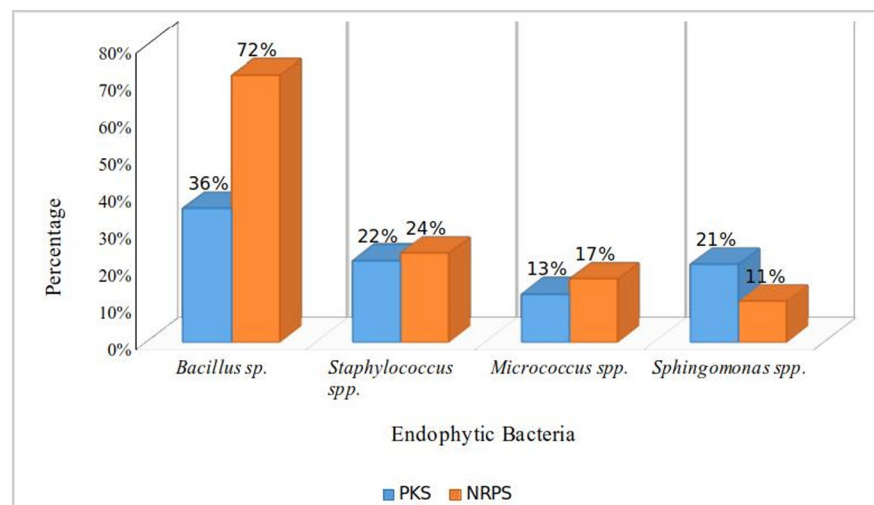


**Fig 10. Distribution of PKS and NRPS domains among the endophytic isolates at the genus level.**

<https://doi.org/10.1371/journal.pone.0269962.g010>

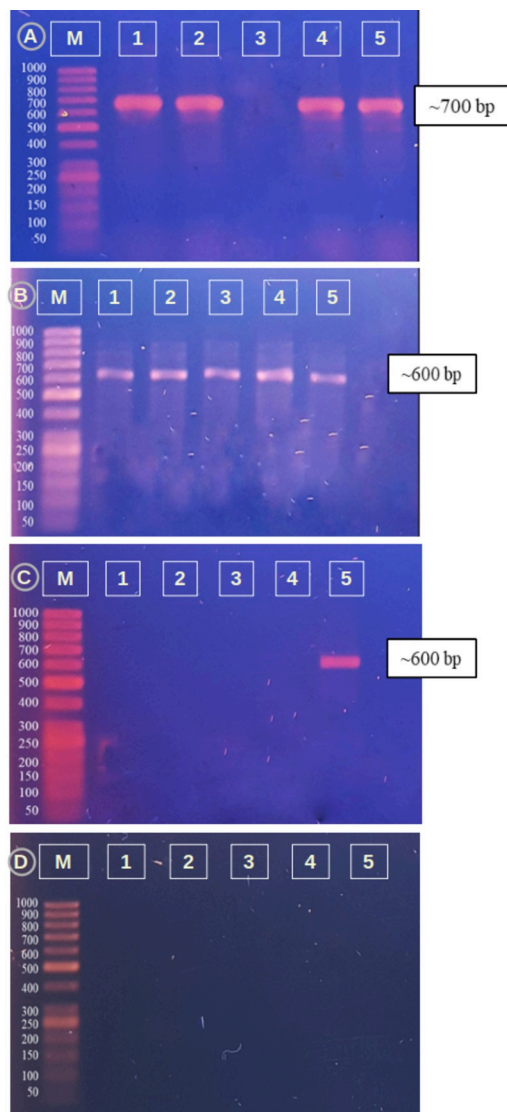


**Fig 11. PCR amplifications of biosynthetic genes.** (A) PKS gene, (B) NRPS gene, (C) ACCD gene and (D) CHS gene. M: DNA Marker for each case; 1: LL1; 2: LL2; 3: LF; 4: GL; 5: GR.

<https://doi.org/10.1371/journal.pone.0269962.g011>

**Table 11. Binding affinities of the reference compound (lopinavir) and other compounds to 3CL<sup>PRO</sup> of coronaviruses.**

Serial no.	Compound/Ligand	Binding Affinity (Kcal/mol)
1.	Lopinavir (ref. compound)	-7.2
2.	Aureusimine	<b>-6.0</b>
3.	Bacitracin	-3.8
4.	Carotenoid	-4.1
5.	Microansamycin	-7.7
6.	Staphyloferrin	-5.8

**Note:** Compounds having the highest binding affinity for the corresponding proteins are the ones indicated in bold values.

<https://doi.org/10.1371/journal.pone.0269962.t011>

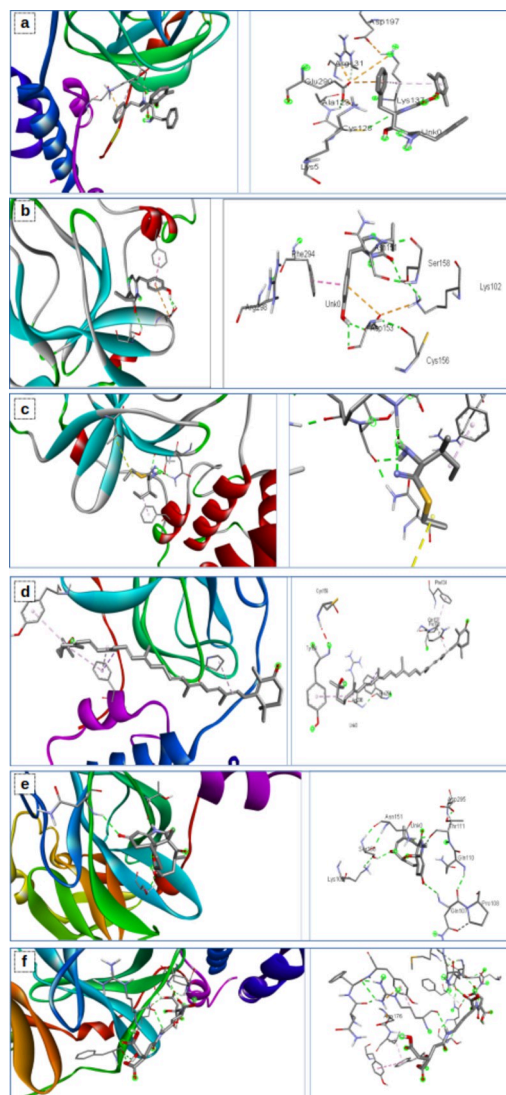


**Fig 12.** Visualization of SARS-CoV-2 3CLpro amino acid interactions with the ligands (A) lopinavir, (B) aureusimine, (C) bacitracin, (D) carotenoid, (E) microanasamycin, and (F) staphyloferrin.

<https://doi.org/10.1371/journal.pone.0269962.g012>

interest in endophytic bacteria until last several years due to their efficacy in mimicking and producing similar bioactive compounds of their respective host plants as well as new bioactive compounds that are not present in host plants [9]. As medicinal plants harbor natural phytochemicals and bioactive compounds, endophytic bacteria within them can be a potential source of interest to investigate natural products [84]. Our study also aims to find a picture of bioactive potentiality inside endophytes by investigating biosynthetic gene clusters and secondary metabolites with molecular studies and *in silico* approaches.

In the subcontinent, approximately 2000 plants with medicinal properties have been reported, and among them, approximately 500 of such medicinal plants have thus far been enlisted as growing or available in Bangladesh [85]. In our study, we collected our plant samples around the campus of Chittagong University (Table 2), as it is a good reservoir of indigenous plants of Bangladesh [85]. As we are interested in identifying culturable endophytic bacteria from various parts of the plants, we collected root, stem, and leaf parts of each plant

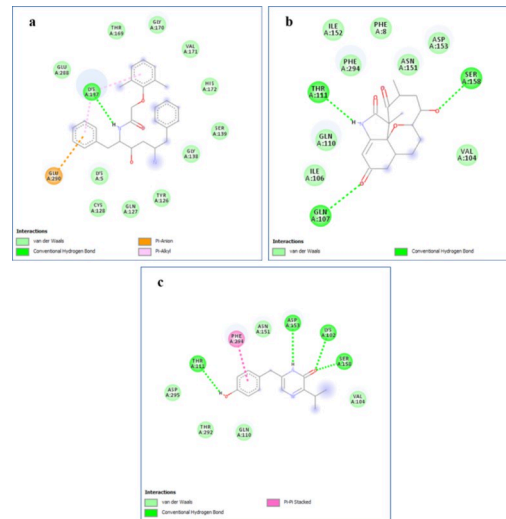


**Fig 13. 2D representation of protein–ligand interactions.** Binding mode of 3CLpro with A) lopinavir, B) microanasamycin, and C) aureusimine.

<https://doi.org/10.1371/journal.pone.0269962.g013>

sample. We did not consider the flower and seed parts, as we selected different herbs, shrubs, and trees to avoid flowering and nonflowering properties [71]. In this study sixteen medicinal plant samples were collected from eight (8) different locations to obtain diversity.

The surface sterilization process was performed carefully to eliminate the epiphytes from the plant parts. Phosphate buffer solution (PBS) was used to triturate the internal plant extracts obtained from the leaves, roots, and stems [65]. The extracts were collected after trituration and then spread on the culture plates of nutrient agar (NA) media through the pour-plate technique [86]. We used nutrient agar (NA) and Luria-Bertani (LB) agar media to study further growth of isolated endophytic bacteria. Thus, 16 bacterial isolates (endophytes) were selected from forty eight medicinal plant parts which confirms the culture-dependent nature of those endophytic bacteria [5, 64]. Colonies were then separated by identifying colony color, shape and orientation for further pure culture (Fig 1) by the streaking method [29, 69]. Standard morphological and biochemical tests were performed to characterize and identify five bacterial isolates, LL1, LL2, LF, GL, and GR [66, 87]. In the case of gram staining study (Table 6), four isolates LL1, LL2, LF, and GL were considered gram-positive because of having cell walls of a thick peptidoglycan layer (50–90%) which stained violate under the microscope; on contrast, a thinner layer of peptidoglycan (less than 10%) was observed which stained pink was found for isolate GR and considered as gram-negative [88]. From the morphological study, LL2 and GL were found to be cocci, and LL1, LF, and GR were found to be rod-shaped bacteria.

LL2 and GL (gram-positive cocci) showed positive results for catalase, oxidase, and methyl red tests (Table 6) which implied that the isolates were either *Staphylococcus spp.* or *Micrococcus spp.* [66, 89]. Following negative results for the indole test and VP test (Table 6), LL2 showed positive results for mannitol salt fermentation (Table 6) whereas GL showed a negative result. Thus, LL2 is strongly assumed to be *Staphylococcus aureus* and GL as *Micrococcus luteus* [65, 90]. Gram-positive rods LL1 and LF showed positive results for catalase, oxidase, and methyl red tests, as well as negative results for indole tests, VP tests, and mannitol salt fermentation (Table 6). Therefore, these two isolates were considered similar to *Bacillus spp.* [66, 91]. Positive test results in the citrate utilization test (Table 6) conferred isolate LL1 to be similar to *Bacillus subtilis*. On the other hand, the gram-negative rod-shaped isolate GR showed

Table 12. Physicochemical properties of the binding compounds.

Lipinski filters analysis						
Lipinski filters	Lopinavir	Aureusimine	Bacitracin	Carotenoid	Microansamycin	Staphyloferrin
Mol. weight (g/mol)	628.80	244.29	1422.69	568.87	319.35	480.38
Num. heavy atoms	46	18	100	42	23	33
Num. rotatable bonds	17	3	35	14	0	18
Num. H-bond acceptors	5	3	20	2	5	14
Num. H-bond donors	4	2	17	1	2	9
Molar Refractivity	187.92	70.91	399.90	188.21	84.24	101.10
Druglikeness						
Lipinski Filter	Yes	Yes	No	No	Yes	No
Ghose	No	Yes	No	No	Yes	No
Veber	No	Yes	No	No	Yes	No
Egan	Yes	Yes	No	No	Yes	No
Muegge	No	Yes	No	No	Yes	No
ADMET analysis (Probability)						
a) Absorption						
Blood-Brain Barrier	+ (0.9104)	+0.9670	+0.9270	+0.9049	+0.9435	+0.9640
Human Intestinal Absorption	+ (0.9624)	+0.9925	+0.8746	+0.9879	+0.9063	-0.6694
Bioavailability Score	0.55	0.55	0.17	0.17	0.55	0.11
Caco-2	+ (0.9313)	+0.7591	-0.8675	-0.7841	+0.5576	-0.8885
P-glycoprotein Substrate	+ (0.7009)	-0.8841	+0.8733	-0.6950	-0.5051	-0.7300
P-glycoprotein Inhibitor	+ (0.9511)	-0.9197	+0.7422	+0.8359	-0.9012	-0.5469
b) Distribution						
Subcellular localization	Mitochondria (0.7846)	Mitochondria (0.8990)	Mitochondria (0.4232)	Mitochondria 0.7289	Mitochondria 0.7657	Mitochondria 0.8125
c) Metabolism						
CYP1A2 inhibition	-(0.8935)	+0.6112	-0.9046	-0.8585	-0.8444	-0.8870
CYP2C9 inhibition	-(0.7326)	-0.8667	-0.9071	-0.8478	-0.8855	-0.9408
CYP2C19 inhibition	-(0.7983)	-0.5533	-0.9025	-0.8443	-0.8605	-0.9215
CYP2D6 inhibition	-(0.9438)	-0.9369	-0.9231	-0.8980	-0.9441	-0.9250
d) Toxicity						
AMES Toxicity	-(0.8300)	-0.8400	-0.6900	-0.8300	-0.7800	-0.7700
Carcinogens	-(0.6710)	-0.9286	-0.8714	-0.6888	-0.9286	-0.9571
Acute Oral Toxicity (kg/mol)	2.994	1.301	3.098	2.967	3.711	2.264
Hepatotoxicity	+(0.7000)	+0.6750	-0.6250	+0.5750	-0.7250	-0.6250
Aqueous solubility (LogS)	-3.414	-2.734	-3.079	-2.078	-3.091	-1.813
e) Pharmacokinetics						
GI absorption	High	High	Low	Low	High	Low
Log Kp (skin permeation) cm/s	-5.93	-6.45	-17.88	-1.14	-8.52	-12.35

<https://doi.org/10.1371/journal.pone.0269962.t012>

negative results for all biochemical tests except the oxidase test. Thus, it is assumed that the isolate was similar to *Pseudomonas spp.* or *Aeromonas spp.* [66].

Antibiotics are natural or semisynthetic drugs used against bacterial infections. A number of antibiotics are in use for medications for a long time; hence, rapid and uncontrolled uses of antibiotics lead to antibiotic resistance. New pathogens have evolved to be resistant to antibiotic action, which creates the need to discover new novel antibiotics [92, 93]. An antibiotic

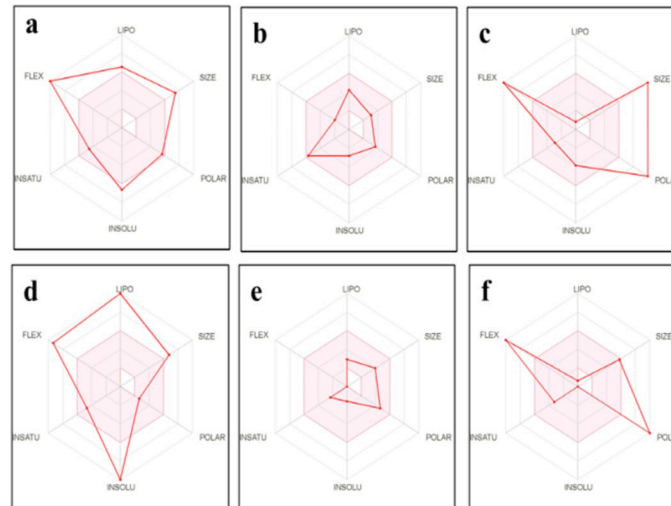


**Fig 14. Summary of the pharmacokinetic properties of the compounds.** (a) Lopinavir, (b) aureusimine, (c) bacitracin, (d) carotenoid, (e) microanamyacin, (f) staphyloferrin The color space is a suitable physicochemical space for oral bioavailability. LIPO Lipophilicity:  $-0.7 < XLOGP3 < +5.0$ . SIZE:  $150 \text{ g/mol} < MW < 500 \text{ g/mol}$ . POLAR (Polarity):  $20 \text{ \AA}^2 < TPSA < 130 \text{ \AA}^2$ . INSOLU (insolubility):  $0 < \text{Log S (ESOL)} < 6$ . INSATU (insaturation):  $0.25 < \text{Fraction Csp3} < 1$ . FLEX (Flexibility):  $0 < \text{Num. rotatable bonds} < 9$ .

<https://doi.org/10.1371/journal.pone.0269962.g014>

sensitivity test was performed to identify suitable antibiotics that will be most effective against the specific type of bacteria. Here, we performed this test to evaluate the most commonly used antibiotics against bacterial isolates to determine the harmful bacterial strains. Ten frequently used antibiotics containing discs (Himedia, India), penicillin G (P), chloramphenicol (C), ampicillin (AMP), streptomycin (S), vancomycin (VA), norfloxacin (NX), tetracycline (TE), nalidixic acid (NA), erythromycin (E), and ceftriaxone (CTR), were used to identify their sensitivity against our five isolated endophytic bacteria (Fig 16). Each isolate showed resistance (R) toward penicillin G. Isolate LL2 also had the highest resistance percentage by showing resistance to tetracycline, erythromycin, and ceftriaxone. LL1 expressed intermediate sensitivity (I) to ampicillin. The rest of the antibiotics were found to be sensitive (S) to other isolated endophytic bacteria. One of the major causes of sensitivity to antibiotics can be the reduced exposure of endophytic bacteria in the human system rather than the inner plant [39, 94, 95].

16S rDNA amplification was conducted through PCR for further confirmatory identification of isolated bacterial species. Genomic DNA was extracted by the conventional method [96], and DNA concentrations were measured by Nanodrop spectroscopy (Thermo Scientific, USA). Then the extracted DNA of five bacterial isolates was amplified by universal 16S rDNA primer pairs [5, 68]. All five isolates showed prominent bands (~800 bp) compared to the 50 bp DNA marker on a 2% agarose gel (Fig 2). In general 16S rDNA and Sanger sequencing (Macrogen's sequencing service, South Korea) were performed to identify the strains of the respective bacterial isolates [97]. Homology analysis inferred from 16S rDNA sequence comparison clearly verified that the five isolates clustered with *Priestia megaterium* (LL1), *Staphylococcus caprae* (LL2), *Neobacillus drentensis* (LF), *Micrococcus yunnanensis* (GL), and *Sphingomonas paucimobilis* (GR) (Table 6) having 99% identity in BLAST analysis [18]. All the results were submitted to GenBank where the accession numbers MW494406 (LL1), MW494408 (LL2), MW494401 (LF), MW494402 (GL), and MZ021340 (GR) were assigned.

Phylogenetic trees were constructed (Fig 3) to determine the similarity with other members of the strains found in homology analysis [71]. Evolutionary analyses were conducted in MEGA 11 [50] using the neighbor-joining method. Only sequences from the type of mostly

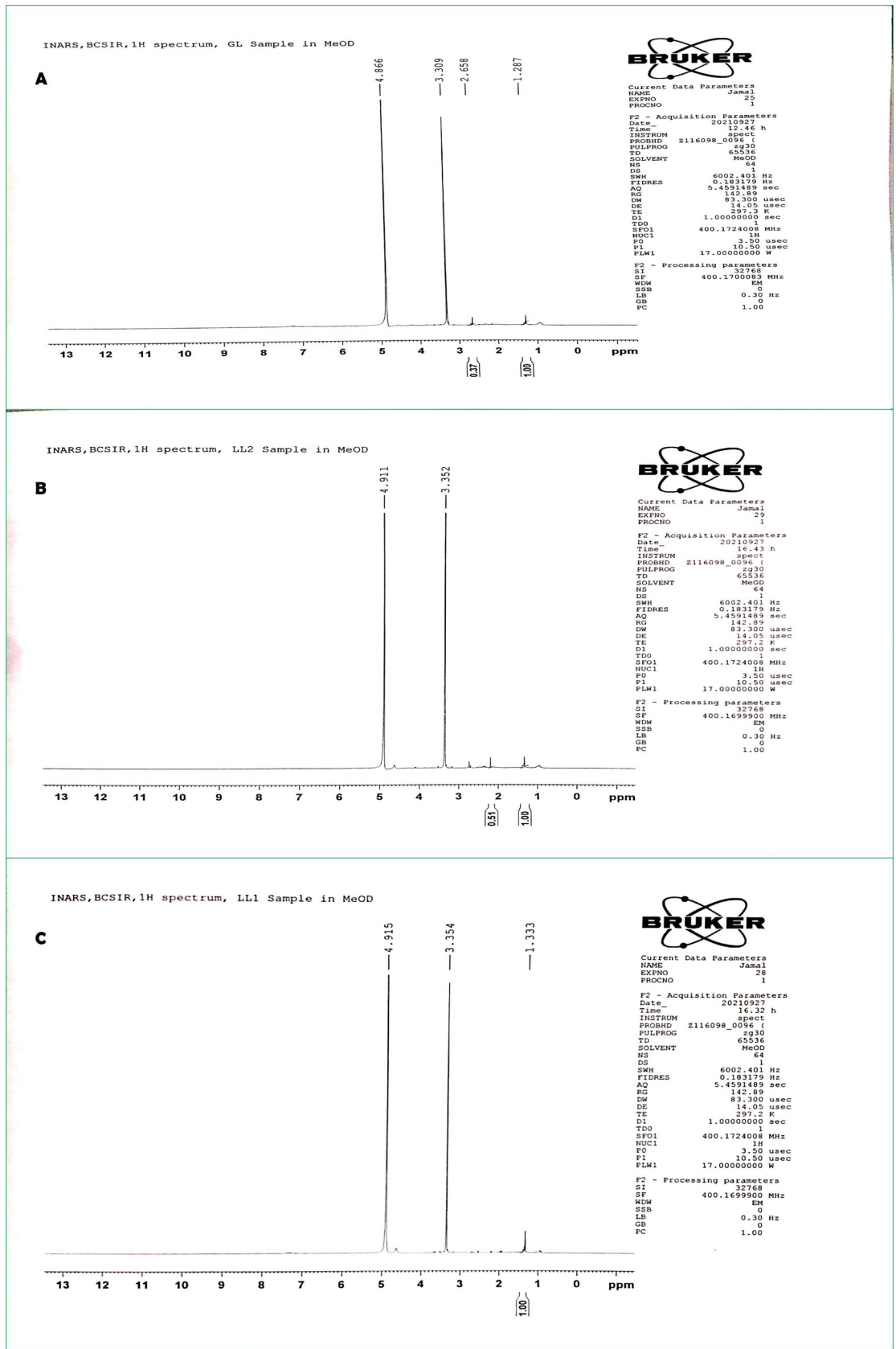


**Fig 15. NMR <sup>1</sup>H spectroscopy result: In the left the metabolite structure and on the right <sup>1</sup>H NMR spectrum.** Every peak is responsible for a respective different proton type. (A) Microansamycin, (B) Aureusimine, and (C) Surfactin.

<https://doi.org/10.1371/journal.pone.0269962.g015>

identical strains were taken into account. More than 200 bacterial genera from 16 phyla have been reported to be associated with endophytes, with the majority of the species belonging to the phyla Actinobacteria, Proteobacteria, and Firmicutes [98]. Our study identified three Firmicutes (*Priestia megaterium*, *Staphylococcus caprae*, and *Neobacillus drentensis*), one actinobacterial (*Micrococcus yunnanensis*), and one proteobacterial (*Sphingomonas paucimobiliz*) endophyte from different medicinal host plants around the Chittagong University campus.

Endophytic bacteria have been reported to play a vital role in growth promotion, nutrient management, disease control, and biotic and abiotic stress tolerance in food and crop plants [9, 99]. Phytohormones play a significant role in plant growth promotion and it was suggested that IAA production helps the plants grow root parts, which increases the plants' nutrient uptake [99]. Five identified isolates were screened for growth-promoting parameters and found positive for indole acetic acid (IAA) production. Quantitative estimation of all isolates was performed in ISP2 broth medium and production ranged from 14.26 µg/mL to 25.561 µg/mL (Table 7). The maximum IAA yield was observed in *Sphingomonas paucimobiliz* (25.561 µg/mL). This finding is similar to Khamna et al. (2009) who stated that IAA production levels ranged from 13.73 µg/ml to 142 µg/ml [71, 100] in bacterial endophytes. Ammonia production is an indirect mechanism of plant growth promotion and can play a significant role in suppressing phytopathogens [101]. In the present study, all isolates showed ammonia production in peptone water broth ranging from 5.3 mg/mL to 24.98 mg/mL (Table 7). Qualitative estimation showed that isolating *Staphylococcus caprae* resulted in the maximum yield of ammonia (24.98 mg/mL). Studies have suggested similar results of ammonia production range

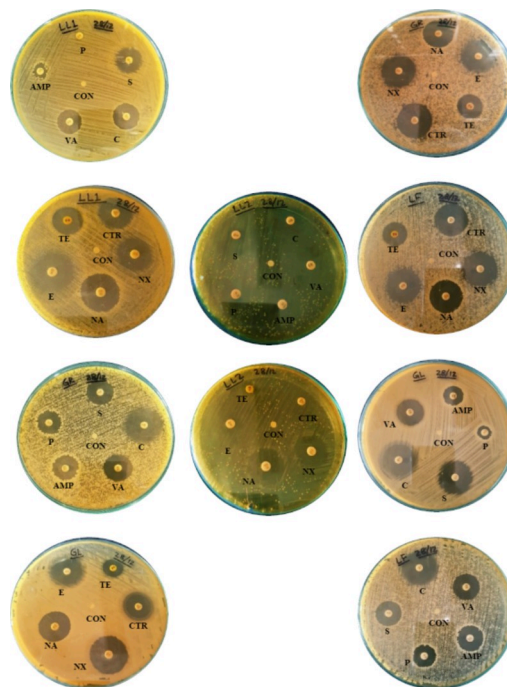


**Fig 16. Antibiotic sensitivity test of isolates showing inhibition zones (mm).** Control (CON) indicates discs without antibiotics in each case. Disc codes are used to show the antibiotic discs for every isolate.

<https://doi.org/10.1371/journal.pone.0269962.g016>

by endophytic bacteria and inferred an association in plant growth promotion [6, 71]. The isolated bacterial strains *Priestia megaterium* (LL1) and *Staphylococcus caprae* (LL2) showed protease positive results by degrading casein in skim milk agar (Fig 5). Previous studies suggested that *Bacillus*, *Paenibacillus*, and *Pseudomonas* are highly recognized as protease producers [8, 63].

Phenolics and flavonoids are responsible for exhibiting the antioxidant properties of chemical compounds. The presence of antioxidant compounds such as total phenolic content (TPC) and total flavonoid content (TFC) in endophytic bacteria and solvent extracts was assessed [89] in the present study. As an extraction solvent, ethyl acetate extract (EA) was used because it is selective in extracting low molecular weight phenols and flavonoids [70]. The highest TPC value was found in *Staphylococcus caprae* ( $406.653 \pm 0.01$   $\mu\text{g/mL}$ ) (Table 7) and it also exhibited the highest TFC value ( $45.18 \pm 0.5$   $\mu\text{g/mL}$ ) (Table 7). The TPC and TFC values found in the present study were higher than those reported in previous studies [70, 102, 103]. Therefore, endophytic *Staphylococcus caprae* could be a source of natural phenolics and flavonoids to act as antioxidant compounds. These compounds also shows antiviral activity against various microorganisms [104, 105]. Moreover, some recent studies presented the efficacy of these compounds against SARS-COV-2 [106].

In recent years, bioactive compounds have been in high demand due to their benefits to humans and plants in various sectors of application. Thus, endophytic bacteria act as a promising resource of biotechnologically valuable bioactive compounds as well as secondary metabolites [107, 108].

Most bacterial secondary metabolites are produced by biosynthetic gene clusters consisting of key enzymes, such as polyketide synthases (PKSs) or non-ribosomal peptide synthetases (NRPSs), and contiguous genes encoding tailoring enzymes and transporters [6]. To explore the biosynthetic gene clusters and their associated bioactive secondary metabolites from our isolated bacterial strains, we used the webserver tool antiSMASH 5.0 bacterial version [109]. With default parameters of input data, we found thirteen different secondary metabolite regions from five isolates (Fig 6). The most abundant regions found were Terpene, Siderophore, and Type III polyketide synthase regions followed by NRPS, Lanthipeptide, and Beta-lactone regions (Fig 7). Among the five isolates, the *Priestia megaterium* strain showed the maximum number of metabolite regions, conferring itself as a potent source of bioactive compounds [19]. The antiSMASH server linked the data with the MIBig server, where we found the information of the most similar known cluster related to the database and represented the features of predicted bioactive compounds [110]. Nine compounds were found to be matched with the database, and structure, features and the list of core biosynthetic genes along with additional and other regulatory genes were retrieved from the results (Table 9). Four nonribosomal peptide (NRP)-type compounds—Surfactin (lipopeptide), Bacitracin, Microansamycin (cyclic desepptide), and Aureusimine—Three terpene type compounds—Carotenoid, Stenothricin, and Zeaxanthin—were identified. The other two compounds were staphyloferrin A (siderophore) and fengycin (betalactone).

Compound results are represented as the most similar known compounds from the BLAST result of the database, in which aureusimine, staphyloferrin A, and zeaxanthin were matched 100% with our query sequences (Fig 8). Thus, *S. caprae* and *S. paucimobilis* can be a great source of antioxidant metabolite extraction for further detailed study of their bioactivity.

Compound structure, features, and information on core and biosynthetic genes involved in the secondary metabolite clusters were also retrieved from the MIBiG server [26]. Later, the genes and protein products were evaluated through the UniProt server to obtain information on proteins, their biological processes, and their biosynthesis pathways (Table 10). Amino acid sequences from the clusters were run through the peptide search of UniProt and the

protein products of the genes were extracted. After that, the STRING server (version 11.0) [72] was used to represent the networks, association, and correlation between the genes and proteins involved in biosynthetic gene clusters [17, 111] (Fig 9). Unfortunately, enough protein data could not be retrieved for aureusimine, microansamycin, and stenothricin from the database to show the interactions.

**Surfactin** is widely known as a biosurfactant along with its antimicrobial properties and has already shown a handful of bioactive potentialities [74]. Defining the genes involved in the surfactin cluster, we found that *srfAA*, *srfAB*, *srfAC*, and *srfAD* were the core genes involved in surfactin biosynthesis (Table 10). *srfAD* is the core gene associated with synthetase genes and the transporter gene *tcyC* to modulate the surfactin biosynthesis pathway. It was shown to be a clear protein–protein interaction of these genes. On the other hand, the additional biosynthetic genes *ycxB* and *ycxCadycxD* encode regulation- and transport-related proteins involved in the processing of this secondary metabolite. Surfactin has shown experimental success due to its antibacterial capacity [112] and inhibitory mechanism against pathogenic bacteria [113]. It has been shown to enhance surfactin production from *B. licheniformis* and *Bacillus amyloliquefaciens* [114], and thus, it is promising to use *Priestia megaterium* as a potential source to synthesize this biosurfactant.

**Bacitracin** is a cyclic polypeptide antimicrobial derived from the bacterium *Bacillus subtilis* that has wide use for the treatment of superficial bacterial skin infections [75]. The bacitracin gene cluster comprises three core biosynthetic genes (*bacA*, *bacB*, and *bacC*) and three additional genes (*bacR*, *bacS*, and *bacT*) (Table 10). From the protein database, it was found that the core bac genes are directly involved in the antibiotic (bacilysin) biosynthesis pathway, conferring that *P. megaterium* possesses such a synthesis pathway. This isolate can be used for metabolic engineering to enhance bacitracin action, as it is now graded as less functional against multidrug-resistant bacteria. No data involved in using endophytic bacteria using bacitracin production have been found previously, and thus, the metabolic engineering strategy to enhance bacitracin production is attractive.

**Carotenoids**, a subfamily of isoprenoids, are among the most widespread, diverse classes of all-natural products and biomolecules. Bacteria synthesize isoprenoids from isopentenylidiphosphate (IPP) and its isomer dimethylallyldiphosphate (DMAPP) through the methylerythritol 4-phosphate (MEP) pathway [115]. The *crtM* gene is the core gene that initiates the biosynthesis pathway [116], which clarifies the central action of the protein network (Table 10). Carotenoids are well-known pigments in plants, algae and photosynthetic bacteria. It is also an antioxidant for humans consumed by foods and fruits.

**Zeaxanthin** is also a carotenoid essential for our eyes against photooxidative damage from UV light. Animals and humans cannot synthesize zeaxanthin, and thus, it must be obtained through diet [117]. Zeaxanthin is supplemented through food, and now, it has increased the commercial demand for production [118]. Endophytic bacteria can be a reliable source for commercially synthesized carotenoids such as zeaxanthin and from this research, the endophytic isolate *S. paucimobilis* can be used as a novel resource for metabolite production [119].

**Fengycin** is a novel antimicrobial agent effective against the fungal community isolated from *B. subtilis* [93]. Twelve different genes distributed in 4 synthetic clusters are responsible for the synthesis of this metabolite. A glycoside hydrolase ( *yngK*) plays a connector role in the regulation of neighborhood nonribosomal synthetase activity (*fenA*, *fenB*, *fenC*,  *fend*) and regulation activity ( *yngE*,  *yngF*,  *yngG*,  *yngH*,  *yngI*,  *yngJ*) of the genes involved in the fengycin synthase pathway (Table 10). Fengycin exhibited strong antifungal activity and inhibited the growth of several plant pathogens, particularly many filamentous fungi [120]; thus, the isolate *Neobacillus dretenensis* can be utilized as a harbor of novel antifungal secondary metabolites. Last, the siderophore compound staphyloferrin A comprises 4 core biosynthetic genes related

to nonribosomal peptide synthetase in the action of siderophore biosynthesis, an important mechanism to overcome iron limitation [121]. It has been used as a detector of multidrug-resistant *Staphylococcus aureus* (MRSA) [6] and can open a new window of research on endophytic bacteria against antibiotic resistance mechanisms.

Most biologically active polyketide and peptide compounds are synthesized by polyketide synthases (PKSs) and nonribosomal peptide synthetases (NRPSs), which have been widely utilized to assess the biosynthetic capacity of culturable and nonculturable bacteria [19, 114, 122]. PKS and NRPS domain occurrence was analyzed for our isolated bacterial strains from the SBSPKS V2 database. The identified strains showed significant PKS and NRPS domain data for evaluating endophytes of biosynthetic potential. Therefore, *Bacillus spp.* represented the highest percentage (PKS 36%, NRPS 72%), whereas *Staphylococcus spp.* (PKS 22%, NRPS 24%), *Micrococcus spp.* (PKS 13%, NRPS 17%) and *Sphingomonas spp.* (PKS 21%, NRPS 11%) having a moderate percentage (Fig 10). This result demonstrated the universal distribution of these domains in terms of the identification of biosynthetic genes for secondary metabolite production [15, 56, 123].

The presence of biosynthetic genes encoding polyketide synthases (PKS), nonribosomal peptide synthetases (NRPS), 1-aminocyclopropane-1-carboxylate deaminase (ACCD), and chalcone synthase (CHS) was analyzed by identifying five strains using four sets of degenerate primers (Table 5). PCR amplification of all five isolates showed a band of the expected size (~700–800 bp) for the NRPS gene (Fig 11B). PKS candidate amplicons (~700–800 bp) were detected in *Priestia megaterium* (LL1), *Staphylococcus caprae* (LL2), *Micrococcus yunnanensis* (GL), and *Sphingomonas paucimobiliz* (GR) (Fig 11A), whereas *Sphingomonas paucimobiliz* (GR) showed only positive amplification of the ACCD gene (Fig 11C). For the CHS gene, no amplicons were found for any endophytic strain (Fig 11D). A putative prospect for bioactive secondary metabolites indicates that the positive strains can be a good candidate to research for natural bioactive compounds [12, 124]. *Sphingomonas paucimobiliz* showed positive results for three of the genes except for ACCD, which indicates its involvement in the pathways of plant-endophytic interaction and may be a reservoir of secondary metabolites [4, 125]. Further research and investigation of these gene and gene clusters may explore the novel bioactive natural products defining endophytic bacteria and their host interaction in medicinal plants [107, 126].

Microbial metabolites have some major advantages over synthetic drugs. Following the failure of numerous conventional medicines to treat viral infections and the emergence of particular viral resistances, interest in microbial metabolites as potential antiviral agents has grown. The recent COVID pandemic also had an immense impact on sorting out the best possible compounds against the deadly coronavirus. To exploit the probable candidate against SARS-COV2, predicted bioactive secondary metabolites were subjected to molecular docking against 3-chymotrypsin-like protease (3CL<sup>Pro</sup>) of SARS-COV2. Out of nine metabolites, five metabolites were used to dock against the target protein, and four of them (surfactin, stenothricin, fen-gycin, and zeaxanthin) were excluded due to the incomplete conformation of their structure. The results from this study revealed that lopinavir, the reference inhibitor, had a binding affinity of -7.2 Kcal/mol for 3CL<sup>Pro</sup> of SARS-COV-2 (Table 11). The two top docked compounds to SARS-COV-2 3CL<sup>Pro</sup> are Microansamycin (-7.7 kcal mol<sup>-1</sup>) and Aureusimine (-6.0 kcal. mol<sup>-1</sup>). The results obtained from the ligand-protein binding interaction showed that lopinavir docked into the receptor-binding site and interacted via a conventional hydrogen bond and Pi-alkyl bond to LYS137. It further interacted with GLU290 via a Pi-Anion bond. This was attributed to multiple noncovalent interactions, such as hydrogen bonds and van der Waals (VDW) interactions, with other amino acid residues (GLU288, THR169, GLY170, VAL171, HIS172, SER139, GLY138, TYR126, GLN127, CYS128, LYS5) at the active site of 3CL<sup>pro</sup> (Fig 13A).

Microansamycin, the topmost docked compound to 3CL<sup>Pro</sup> of SARS-COV-2, interacted via three conventional hydrogen bonds to the GLN107, THR111, and SER158 residues, along with VDW noncovalent interactions with ILE106, GLN110, PHE294, ILE152, PHE, ASN151, ASP153, and VAL104 amino acid residues (Fig 13B).

Aureusimine interacted with PHE294 via a Pi-Pi stacked interaction along with four conventional hydrogen bonds, THR111, ASP153, LYS102, and SER158, of 3CL<sup>Pro</sup>. The other VDW bonds were ASP295, THR292, GLN110, ASN151, and VAL104 (Fig 13C).

These with a possible inhibitory propensity against the SARS coronavirus were identified based on the findings of these docking results. The stronger interactions of these two with 3CLpro compared to the reference compound imply that they may alter the viral protease function, which is required for the processing of viral replicase polyproteins.

To validate our prediction of being a potential drug, we analyzed the pharmacokinetic properties of the docked compounds (Table 12). According to Lipinski's rule, an orally active medication cannot contain more than one violation of the following conditions: Not >5 hydrogen bond donors (oxygen or nitrogen atoms with one or more hydrogen atoms); Not >10 hydrogen bond acceptors (nitrogen or oxygen atoms); A molecular mass <500 Daltons; and an octanol-water partition coefficient (logP) not greater than 5. Microansamycin and aureusimine fulfilled the requirements with corresponding favorable predicted ADMET parameters (Fig 14). The five compounds' anticipated filtering analyses revealed characteristics that point to favorable ADME/tox and pharmacokinetic capabilities. This also suggests that the best-docked compounds (microansamycin and aureusimine) have drug potentiality. However, we have found microansamycin, aureusimine, and stenothricin through NMR results (Fig 15) that were present in the bacterial crude extract. Both microansamycin and aureusimine show various bioactivities including antibacterial, antiviral, antifungal, antitumor, and immunosuppressive [127, 128]. Hence, our study also revealed the antiviral potentiality of those metabolites by using different computational tools. This might be a harbinger of a structure-based medication design for COVID-19 that targets the 3CL<sup>Pro</sup> of SARS-COV-2. Therefore, antiviral microbial metabolites may present a significant opportunity in the field of pharmaceutical research and development in the near future, and endophytic bacterial bioactive compounds can be a rich source of natural products.

## Conclusion

This study revealed that endophytic bacterial secondary metabolites could be used as valuable bioactive compounds against disease-causing pathogens. Our study also suggests that the endophytic bacterial bioactive compounds microansamycin and aureusimine expose pharmaceutical efficacy targeting 3CLpro of SARS-COV-2 which represents a potential ingredient for pharmaceutical applications with antiviral properties and are worthy of future study for medication against SARS-COV-2.

## Supporting information

**S1 Raw images. Electrophoretic separation (2% agarose) of the 16S rDNA gene of different isolates.**

(TIF)

**S2 Raw images. PCR amplifications of biosynthetic genes. (C) ACCD gene.**

(TIF)

**S3 Raw images. PCR amplifications of biosynthetic genes. (D) CHS gene (No Result).**

(TIF)

**S4 Raw images. PCR amplifications of biosynthetic genes.** (B) NRPS gene.  
(TIF)

**S5 Raw images. PCR amplifications of biosynthetic genes.** (A) PKS gene.  
(TIF)

**S1 Fig. All the compounds' structures in 3D.**  
(DOCX)

## Acknowledgments

This study was partially supported by the Research & Publication Cell of the University of Chittagong, Bangladesh, and the Ministry of Science and Technology, Government of the people's republic of Bangladesh (Special Allocation). This research was done in the 'Molecular Biology Laboratory' of the Department of Genetic Engineering and Biotechnology, University of Chittagong. The authors are pleased to mention the valuable suggestions during this research from Professor Kazuyuki Shimizu, Department of Bioscience & Bioinformatics, Kyushu Institute of Technology, Iizuka, Fukuoka 820–8502, Japan, and Institute of Advanced Bioscience, Keio University, Tsuruoka, Yamagata 997–0017, Japan. The research team is pleased to acknowledge the Bangladesh Council of Scientific and Industrial Research (BCSIR), DHAKA, Bangladesh for NMR detection.

## Author Contributions

**Conceptualization:** Lolo Wal Marzan.

**Data curation:** Yasmin Akter, Rocktim Barua, Md. Nasir Uddin.

**Formal analysis:** Abul Fazal Muhammad Sanaullah, Lolo Wal Marzan.

**Funding acquisition:** Lolo Wal Marzan.

**Investigation:** Yasmin Akter, Rocktim Barua, Md. Nasir Uddin.

**Methodology:** Yasmin Akter, Rocktim Barua, Md. Nasir Uddin.

**Supervision:** Yasmin Akter, Lolo Wal Marzan.

**Writing – original draft:** Rocktim Barua.

**Writing – review & editing:** Yasmin Akter, Md. Nasir Uddin, Lolo Wal Marzan.

## References

1. Schulz B. Mutualistic interactions with fungal root endophytes. *Microbial root endophytes*. Springer; 2006. pp. 261–279.
2. Wilson D. Endophyte: the evolution of a term, and clarification of its use and definition. *Oikos*. 1995; 274–276.
3. Zhang HW, Song YC, Tan RX. Biology and chemistry of endophytes. *Nat Prod Rep*. 2006; 23: 753–771. <https://doi.org/10.1039/b609472b> PMID: 17003908
4. Santoyo G, Moreno-Hagelsieb G, del Carmen Orozco-Mosqueda M, Glick BR. Plant growth-promoting bacterial endophytes. *Microbiol Res*. 2016; 183: 92–99. <https://doi.org/10.1016/j.micres.2015.11.008> PMID: 26805622
5. Wang S-S, Liu J-M, Sun J, Sun Y-F, Liu J-N, Jia N, et al. Diversity of culture-independent bacteria and antimicrobial activity of culturable endophytic bacteria isolated from different *Dendrobium* stems. *Sci Rep*. 2019; 9: 1–12.
6. Singh M, Kumar A, Singh R, Pandey KD. Endophytic bacteria: a new source of bioactive compounds. *3 Biotech*. 2017; 7: 1–14.

7. Vandana UK, Rajkumari J, Singha LP, Satish L, Alavilli H, Sudheer PDVN, et al. The Endophytic Microbiome as a Hotspot of Synergistic Interactions, with Prospects of Plant Growth Promotion. *Biology (Basel)*. 2021; 10: 101. <https://doi.org/10.3390/biology10020101> PMID: 33535706
8. Ek-Ramos MJ, Gomez-Flores R, Orozco-Flores AA, Rodríguez-Padilla C, González-Ochoa G, Tamez-Guerra P. Bioactive products from plant-endophytic Gram-positive bacteria. *Front Microbiol*. 2019; 10: 463. <https://doi.org/10.3389/fmicb.2019.00463> PMID: 30984118
9. Ryan RP, Germaine K, Franks A, Ryan DJ, Dowling DN. Bacterial endophytes: recent developments and applications. *FEMS Microbiol Lett*. 2008; 278: 1–9. <https://doi.org/10.1111/j.1574-6968.2007.00918.x> PMID: 18034833
10. Kandel SL, Joubert PM, Doty SL. Bacterial endophyte colonization and distribution within plants. *Microorganisms*. 2017; 5: 77.
11. Pinski A, Betekhtin A, Hupert-Kocurek K, Mur LAJ, Hasterok R. Defining the genetic basis of plant–endophytic bacteria interactions. *Int J Mol Sci*. 2019; 20: 1947. <https://doi.org/10.3390/ijms20081947> PMID: 31010043
12. Brader G, Compant S, Mitter B, Trognitz F, Sessitsch A. Metabolic potential of endophytic bacteria. *Curr Opin Biotechnol*. 2014; 27: 30–37. <https://doi.org/10.1016/j.copbio.2013.09.012> PMID: 24863894
13. Wu W, Chen W, Liu S, Wu J, Zhu Y, Qin L, et al. Beneficial Relationships Between Endophytic Bacteria and Medicinal Plants. *Front Plant Sci*. 2021; 12: 758. <https://doi.org/10.3389/fpls.2021.646146> PMID: 33968103
14. Castronovo LM, Vassallo A, Mengoni A, Miceli E, Bogani P, Firenzuoli F, et al. Medicinal plants and their bacterial microbiota: a review on antimicrobial compounds production for plant and human health. *Pathogens*. 2021; 10: 106. <https://doi.org/10.3390/pathogens10020106> PMID: 33498987
15. Lee N, Hwang S, Kim J, Cho S, Palsson B, Cho B-K. Mini review: genome mining approaches for the identification of secondary metabolite biosynthetic gene clusters in *Streptomyces*. *Comput Struct Biotechnol J*. 2020; 18: 1548–1556. <https://doi.org/10.1016/j.csbj.2020.06.024> PMID: 32637051
16. Ali S, Duan J, Charles TC, Glick BR. A bioinformatics approach to the determination of genes involved in endophytic behavior in *Burkholderia* spp. *J Theor Biol*. 2014; 343: 193–198. <https://doi.org/10.1016/j.jtbi.2013.10.007> PMID: 24513137
17. Cairns T, Meyer V. In silico prediction and characterization of secondary metabolite biosynthetic gene clusters in the wheat pathogen *Zymoseptoria tritici*. *BMC Genomics*. 2017; 18: 1–16.
18. Kaul S, Sharma T, K Dhar M. “Omics” tools for better understanding the plant–endophyte interactions. *Front Plant Sci*. 2016; 7: 955. <https://doi.org/10.3389/fpls.2016.00955> PMID: 27446181
19. Othoum G, Bougouffa S, Razali R, Bokhari A, Alamoudi S, Antunes A, et al. In silico exploration of Red Sea *Bacillus* genomes for natural product biosynthetic gene clusters. *BMC Genomics*. 2018; 19: 1–11.
20. Contreras-Pérez M, Hernández-Salmerón J, Rojas-Solís D, Rocha-Granados C, del Carmen Orozco-Mosqueda M, Parra-Cota FI, et al. Draft genome analysis of the endophyte, *Bacillus toyonensis* COPE52, a blueberry (*Vaccinium* spp. var. *Biloxi*) growth-promoting bacterium. *3 Biotech*. 2019; 9: 1–6.
21. Demain AL, Sanchez S. Microbial drug discovery: 80 years of progress. *J Antibiot (Tokyo)*. 2009; 62: 5–16. <https://doi.org/10.1038/ja.2008.16> PMID: 19132062
22. Selim KA, Elkhateeb WA, Tawila AM, El-Beih AA, Abdel-Rahman TM, El-Diwany AI, et al. Antiviral and antioxidant potential of fungal endophytes of Egyptian medicinal plants. *Fermentation*. 2018; 4: 49.
23. Halouska S, Zhang B, Gaupp R, Lei S, Snell E, Fenton RJ, et al. Revisiting Protocols for the NMR Analysis of Bacterial Metabolomes. *J Integr OMICS*. 2013; 3: 120–137. <https://doi.org/10.5584/jiomics.v3i2.139> PMID: 26078915
24. Palama TL, Canard I, Rautureau GJP, Mirande C, Chatellier S, Elena-Herrmann B. Identification of bacterial species by untargeted NMR spectroscopy of the exo-metabolome. *Analyst*. 2016; 141: 4558–4561. <https://doi.org/10.1039/c6an00393a> PMID: 27349704
25. Dona AC, Kyriakides M, Scott F, Shephard EA, Varshavi D, Veselkov K, et al. A guide to the identification of metabolites in NMR-based metabolomics/metabolomics experiments. *Comput Struct Biotechnol J*. 2016; 14: 135–153. <https://doi.org/10.1016/j.csbj.2016.02.005> PMID: 27087910
26. Zhu N, Zhang D, Wang W, Li X, Yang B, Song J, et al. A novel coronavirus from patients with pneumonia in China, 2019. *N Engl J Med*. 2020. <https://doi.org/10.1056/NEJMoa2001017> PMID: 31978945
27. Goris T, Pérez-Valero Á, Martínez I, Yi D, Fernández-Calleja L, San Leon D, et al. Repositioning microbial biotechnology against COVID-19: the case of microbial production of flavonoids. *Microb Biotechnol*. 2021; 14: 94–110. <https://doi.org/10.1111/1751-7915.13675> PMID: 33047877
28. Xu L-L, Han T, Wu J-Z, Zhang Q-Y, Zhang H, Huang B-K, et al. Comparative research of chemical constituents, antifungal and antitumor properties of ether extracts of Panax ginseng and its endophytic fungus. *Phytomedicine*. 2009; 16: 609–616. <https://doi.org/10.1016/j.phymed.2009.03.014> PMID: 19403293

29. Gouda S, Das G, Sen SK, Shin H-S, Patra JK. Endophytes: A Treasure House of Bioactive Compounds of Medicinal Importance. *Frontiers in Microbiology*. 2016. p. 1538. Available: <https://www.frontiersin.org/article/10.3389/fmicb.2016.01538> <https://doi.org/10.3389/fmicb.2016.01538> PMID: 27746767
30. Raihan T, Azad AK, Ahmed J, Shepon MR, Dey P, Chowdhury N, et al. Extracellular metabolites of endophytic fungi from *Azadirachta indica* inhibit multidrug-resistant bacteria and phytopathogens. *Future Microbiol*. 2021; 16: 557–576. <https://doi.org/10.2217/fmb-2020-0259> PMID: 33998269
31. Aanouz I, Belhassan A, El-Khatibi K, Lakhlifi T, El-Ldrissi M, Bouachrine M. Moroccan Medicinal plants as inhibitors against SARS-CoV-2 main protease: Computational investigations. *J Biomol Struct Dyn*. 2021; 39: 2971–2979. <https://doi.org/10.1080/07391102.2020.1758790> PMID: 32306860
32. Boopathi S, Poma AB, Kolandaivel P. Novel 2019 coronavirus structure, mechanism of action, antiviral drug promises and rule out against its treatment. *J Biomol Struct Dyn*. 2021; 39: 3409–3418. <https://doi.org/10.1080/07391102.2020.1758788> PMID: 32306836
33. Khan SA, Zia K, Ashraf S, Uddin R, Ul-Haq Z. Identification of chymotrypsin-like protease inhibitors of SARS-CoV-2 via integrated computational approach. *J Biomol Struct Dyn*. 2021; 39: 2607–2616. <https://doi.org/10.1080/07391102.2020.1751298> PMID: 32238094
34. Chen C, Yu X, Kuo C, Min J, Chen S, Ma L, et al. Overview of antiviral drug candidates targeting coronavirus 3C-like main proteases. *FEBS J*. 2021. <https://doi.org/10.1111/febs.15696> PMID: 33400393
35. Jo S, Kim S, Shin DH, Kim M-S. Inhibition of SARS-CoV 3CL protease by flavonoids. *J Enzyme Inhib Med Chem*. 2020; 35: 145–151. <https://doi.org/10.1080/14756366.2019.1690480> PMID: 31724441
36. Xia S, Lan Q, Su S, Wang X, Xu W, Liu Z, et al. The role of furin cleavage site in SARS-CoV-2 spike protein-mediated membrane fusion in the presence or absence of trypsin. *Signal Transduct Target Ther*. 2020; 5: 1–3.
37. Ferreira A, Quecine MC, Lacava PT, Oda S, Azevedo JL, Araújo WL. Diversity of endophytic bacteria from *Eucalyptus* species seeds and colonization of seedlings by *Pantoea agglomerans*. *FEMS Microbiol Lett*. 2008; 287: 8–14. <https://doi.org/10.1111/j.1574-6968.2008.01258.x> PMID: 18710397
38. Addisu D, Kiros L. Isolation and identification of bacteria from fresh fruit juices prepared in cafeterias and restaurants, Axum Town. *Int J Integr Sci Innov Tech*. 2016; 5: 5–10.
39. Liotti RG, da Silva Figueiredo MI, da Silva GF, de Mendonça EAF, Soares MA. Diversity of cultivable bacterial endophytes in *Paullinia cupana* and their potential for plant growth promotion and phytopathogen control. *Microbiol Res*. 2018; 207: 8–18. <https://doi.org/10.1016/j.micres.2017.10.011> PMID: 29458872
40. Castillo U, Harper JK, Strobel GA, Sears J, Alesi K, Ford E, et al. Kakadumycins, novel antibiotics from *Streptomyces* sp. NRRL 30566, an endophyte of *Grevillea pteridifolia*. *FEMS Microbiol Lett*. 2003; 224: 183–190.
41. Beiranvand M, Amin M, Hashemi-Shahraki A, Romani B, Yaghoubi S, Sadeghi P. Antimicrobial activity of endophytic bacterial populations isolated from medical plants of Iran. *Iran J Microbiol*. 2017; 9: 11. PMID: 28775818
42. Steel KJ, Barrow GI, Feltham RKA. *Cowan and Steel's manual for the identification of medical bacteria*. Cambridge university press; 1993.
43. Claus D. The genus *Bacillus*. *Bergey's Man Syst Bacteriol*. 1986; 2: 1105–1139.
44. Bauer AW. Antibiotic susceptibility testing by a standardized single disc method. *Am J clin pathol*. 1966; 45: 149–158.
45. Wayne PA. *Clinical and laboratory standards institute. Performance standards for antimicrobial susceptibility testing*. 2011.
46. Lázaro-Silva DN, De Mattos JCP, Castro HC, Alves GG, Amorim LMF. The use of DNA extraction for molecular biology and biotechnology training: a practical and alternative approach. *Creat Educ*. 2015; 6: 762.
47. Fouad AF, Barry J, Caimano M, Clawson M, Zhu Q, Carver R, et al. PCR-based identification of bacteria associated with endodontic infections. *J Clin Microbiol*. 2002; 40: 3223–3231. <https://doi.org/10.1128/JCM.40.9.3223-3231.2002> PMID: 12202557
48. Mina SA, Marzan LW, Sultana T, Akter Y. Quality assessment of commercially supplied drinking jar water in Chittagong City, Bangladesh. *Appl water Sci*. 2018; 8: 1–8.
49. Johnson M, Zaretskaya I, Raytselis Y, Merezuk Y, McGinnis S, Madden TL. NCBI BLAST: a better web interface. *Nucleic Acids Res*. 2008; 36: W5–W9. <https://doi.org/10.1093/nar/gkn201> PMID: 18440982
50. Tamura K, Stecher G, Kumar S. MEGA11: molecular evolutionary genetics analysis version 11. *Mol Biol Evol*. 2021; 38: 3022–3027. <https://doi.org/10.1093/molbev/msab120> PMID: 33892491

51. Tamura K, Nei M, Kumar S. Prospects for inferring very large phylogenies by using the neighbor-joining method. *Proc Natl Acad Sci*. 2004; 101: 11030–11035. <https://doi.org/10.1073/pnas.0404206101> PMID: 15258291
52. Deljou A, Goudarzi S. Green extracellular synthesis of the silver nanoparticles using thermophilic *Bacillus* sp. AZ1 and its antimicrobial activity against several human pathogenetic bacteria. *Iran J Biotechnol*. 2016; 14: 25. <https://doi.org/10.15171/ijb.1259> PMID: 28959323
53. Singleton VL, Orthofer R, Lamuela-Raventós RM. [14] Analysis of total phenols and other oxidation substrates and antioxidants by means of folin-ciocalteu reagent. *Methods Enzymol*. 1999; 299: 152–178.
54. Chang C-C, Yang M-H, Wen H-M, Chern J-C. Estimation of total flavonoid content in propolis by two complementary colorimetric methods. *J food drug Anal*. 2002;10.
55. Anand S, Prasad MVR, Yadav G, Kumar N, Shehara J, Ansari MZ, et al. SBSPKS: structure based sequence analysis of polyketide synthases. *Nucleic Acids Res*. 2010; 38: W487–W496. <https://doi.org/10.1093/nar/gkq340> PMID: 20444870
56. Ayuso-Sacido A, Genilloud O. New PCR primers for the screening of NRPS and PKS-I systems in actinomycetes: detection and distribution of these biosynthetic gene sequences in major taxonomic groups. *Microb Ecol*. 2005; 49: 10–24. <https://doi.org/10.1007/s00248-004-0249-6> PMID: 15614464
57. Berman HM, Westbrook J, Feng Z, Gilliland G, Bhat TN, Weissig H, et al. The protein data bank. *Nucleic Acids Res*. 2000; 28: 235–242. <https://doi.org/10.1093/nar/28.1.235> PMID: 10592235
58. Liu X, Zhang B, Jin Z, Yang H, Rao Z. The crystal structure of 2019-nCoV main protease in complex with an inhibitor N3. *RCSB Protein Data Bank*. 2020;10.
59. Morris GM, Huey R, Lindstrom W, Sanner MF, Belew RK, Goodsell DS, et al. AutoDock4 and AutoDockTools4: Automated docking with selective receptor flexibility. *J Comput Chem*. 2009; 30: 2785–2791. <https://doi.org/10.1002/jcc.21256> PMID: 19399780
60. Kim S, Chen J, Cheng T, Gindulyte A, He J, He S, et al. PubChem in 2021: new data content and improved web interfaces. *Nucleic Acids Res*. 2021; 49: D1388–D1395. <https://doi.org/10.1093/nar/gkaa971> PMID: 33151290
61. Cheng F, Li W, Zhou Y, Shen J, Wu Z, Liu G, et al. admetSAR: A Comprehensive Source and Free Tool for Assessment of Chemical ADMET Properties. *J Chem Inf Model*. 2012; 52: 3099–3105. <https://doi.org/10.1021/ci300367a> PMID: 23092397
62. Daina A, Michielin O, Zoete V. SwissADME: a free web tool to evaluate pharmacokinetics, drug-likeness and medicinal chemistry friendliness of small molecules. *Sci Rep*. 2017; 7: 42717. <https://doi.org/10.1038/srep42717> PMID: 28256516
63. Erjaee Z, Shekarforoush SS, Hosseinzadeh S. Identification of endophytic bacteria in medicinal plants and their antifungal activities against food spoilage fungi. *J Food Sci Technol*. 2019; 56: 5262–5270. <https://doi.org/10.1007/s13197-019-03995-0> PMID: 31749473
64. Liu Y-H, Guo J-W, Salam N, Li L, Zhang Y-G, Han J, et al. Culturable endophytic bacteria associated with medicinal plant *Ferula songorica*: molecular phylogeny, distribution and screening for industrially important traits. *3 Biotech*. 2016; 6: 1–9.
65. Marzan LW, Alam R, Hossain MA. Characterization, identification and antibiogram studies of endophytic bacteria from cowpea [*Vigna unguiculata* (L.) Walp]. *Bangladesh J Agric Res*. 2018; 43: 175–186.
66. Bergey DH, Holt JG, Krieg P. *Bergey's Manual of Determinative Bacteriology* (1994). Williams Wilkins, Balt MD, USA. 1994.
67. Reller LB, Weinstein M, Jorgensen JH, Ferraro MJ. Antimicrobial susceptibility testing: a review of general principles and contemporary practices. *Clin Infect Dis*. 2009; 49: 1749–1755. <https://doi.org/10.1086/647952> PMID: 19857164
68. Shan W, Zhou Y, Liu H, Yu X. Endophytic actinomycetes from tea plants (*Camellia sinensis*): isolation, abundance, antimicrobial, and plant-growth-promoting activities. *Biomed Res Int*. 2018;2018.
69. Parthasarathy A, Gan HM, Wong NH, Savka MA, Steiner KK, Henry KR, et al. Isolation and genomic characterization of six endophytic bacteria isolated from *Saccharum* sp (sugarcane): Insights into antibiotic, secondary metabolite and quorum sensing metabolism. *J genomics*. 2018; 6: 117. <https://doi.org/10.7150/jgen.28335> PMID: 30310525
70. Monowar T, Rahman M, Bhore SJ, Raju G, Sathasivam K V. Secondary metabolites profiling of *Acinetobacter baumannii* associated with chili (*Capsicum annuum* L.) leaves and concentration dependent antioxidant and prooxidant properties. *Biomed Res Int*. 2019;2019. <https://doi.org/10.1155/2019/6951927> PMID: 30868071
71. Passari AK, Mishra VK, Singh G, Singh P, Kumar B, Gupta VK, et al. Insights into the functionality of endophytic actinobacteria with a focus on their biosynthetic potential and secondary metabolites production. *Sci Rep*. 2017; 7: 1–17.

72. Szklarczyk D, Gable AL, Lyon D, Junge A, Wyder S, Huerta-Cepas J, et al. STRING v11: protein–protein association networks with increased coverage, supporting functional discovery in genome-wide experimental datasets. *Nucleic Acids Res.* 2019; 47: D607–D613. <https://doi.org/10.1093/nar/gky1131> PMID: 30476243
73. Consortium TU. UniProt: the universal protein knowledgebase in 2021. *Nucleic Acids Res.* 2021; 49: D480–D489. <https://doi.org/10.1093/nar/gkaa1100> PMID: 33237286
74. Santos VSV, Silveira E, Pereira BB. Toxicity and applications of surfactin for health and environmental biotechnology. *J Toxicol Environ Heal Part B.* 2018; 21: 382–399. <https://doi.org/10.1080/10937404.2018.1564712> PMID: 30614421
75. Williamson DA, Carter GP, Howden BP. Current and emerging topical antibacterials and antiseptics: agents, action, and resistance patterns. *Clin Microbiol Rev.* 2017; 30: 827–860. <https://doi.org/10.1128/CMR.00112-16> PMID: 28592405
76. Johnson EA, Schroeder WA. Microbial carotenoids. *Downstr Process biosurfactants carotenoids.* 1995; 119–178.
77. Wang J, Li W, Wang H, Lu C. Pentaketide ansamycin microansamycins A–I from *Micromonospora* sp. reveal diverse post-PKS modifications. *Org Lett.* 2018; 20: 1058–1061. <https://doi.org/10.1021/acs.orglett.7b04018> PMID: 29412682
78. Hasenböhler A, Kneifel H, König WA, Zähner H, Zeiler HJ. [Metabolic products of microorganisms. 134. Stenothricin, a new inhibitor of the bacterial cell wall synthesis (author's transl)]. *Arch Microbiol.* 1974; 99: 307–321. <https://doi.org/10.1007/BF00696245> PMID: 4215397
79. Secor PR, Jennings LK, James GA, Kirker KR, deLancey Pulcini E, McInerney K, et al. Phevalin (aureusimine B) production by *Staphylococcus aureus* biofilm and impacts on human keratinocyte gene expression. *PLoS One.* 2012; 7: e40973. <https://doi.org/10.1371/journal.pone.0040973> PMID: 22808288
80. Milner SJ, Seve A, Snelling AM, Thomas GH, Kerr KG, Routledge A, et al. Staphyloferrin A as siderophore-component in fluoroquinolone-based Trojan horse antibiotics. *Org Biomol Chem.* 2013; 11: 3461–3468. <https://doi.org/10.1039/c3ob40162f> PMID: 23575952
81. Kaspar F, Neubauer P, Gimpel M. Bioactive secondary metabolites from *Bacillus subtilis*: a comprehensive review. *J Nat Prod.* 2019; 82: 2038–2053. <https://doi.org/10.1021/acs.jnatprod.9b00110> PMID: 31287310
82. Demmig-Adams B, López-Pozo M, Stewart JJ, Adams WW. Zeaxanthin and lutein: Photoprotectors, anti-inflammatories, and brain food. *Molecules.* 2020; 25: 3607.
83. Cimermancic P, Medema MH, Claesen J, Kurita K, Brown LCW, Mavrommatis K, et al. Insights into secondary metabolism from a global analysis of prokaryotic biosynthetic gene clusters. *Cell.* 2014; 158: 412–421. <https://doi.org/10.1016/j.cell.2014.06.034> PMID: 25036635
84. Liu T, Zhang X, Tian S, Chen L, Yuan J. Bioinformatics analysis of endophytic bacteria related to berberine in the Chinese medicinal plant *Coptis teeta* Wall. *3 Biotech.* 2020; 10: 1–12.
85. Bardhan S, Ashrafi S, Saha T. Commonly Used Medicinal Plants in Bangladesh to treat Different Infections. *J Immunol Microbiol.* 2018; 2: 1–4.
86. Hardoim PR, van Overbeek LS, Elsas JD van. Properties of bacterial endophytes and their proposed role in plant growth. *Trends Microbiol.* 2008; 16: 463–471. <https://doi.org/10.1016/j.tim.2008.07.008> PMID: 18789693
87. Palanichamy P, Krishnamoorthy G, Kannan S, Marudhamuthu M. Bioactive potential of secondary metabolites derived from medicinal plant endophytes. *Egypt J Basic Appl Sci.* 2018; 5: 303–312. <https://doi.org/10.1016/j.ejbas.2018.07.002>
88. Gram C. The differential staining of Schizomycetes in tissue sections and in dried preparations. *Fortschritte der Med.* 1884; 2: 185–189.
89. Ranjan R, Jadeja V. Isolation, characterization and chromatography based purification of antibacterial compound isolated from rare endophytic actinomycetes *Micrococcus yunnanensis*. *J Pharm Anal.* 2017; 7: 343–347. <https://doi.org/10.1016/j.jpha.2017.05.001> PMID: 29404059
90. Prakash O, Nimonkar Y, Munot H, Sharma A, Vemuluri VR, Chavadar MS, et al. Description of *Micrococcus aloeverae* sp. nov., an endophytic actinobacterium isolated from *Aloe vera*. *Int J Syst Evol Microbiol.* 2014; 64: 3427–3433. <https://doi.org/10.1099/ijs.0.063339-0> PMID: 25048212
91. Rat A, Naranjo HD, Krigas N, Grigoriadou K, Maloupa E, Alonso AV, et al. Endophytic Bacteria From the Roots of the Medicinal Plant *Alkanna tinctoria* Tausch (Boraginaceae): Exploration of Plant Growth Promoting Properties and Potential Role in the Production of Plant Secondary Metabolites. *Front Microbiol.* 2021; 12: 113. <https://doi.org/10.3389/fmicb.2021.633488> PMID: 33633713
92. Aswani R, Jishma P, Radhakrishnan EK. Endophytic bacteria from the medicinal plants and their potential applications. *Microbial Endophytes.* Elsevier; 2020. pp. 15–36.

93. Vanittanakom N, Loeffler W, Koch U, Jung G. Fengycin—a novel antifungal lipopeptide antibiotic produced by *Bacillus subtilis* F-29-3. *J Antibiot (Tokyo)*. 1986; 39: 888–901. <https://doi.org/10.7164/antibiotics.39.888> PMID: 3093430
94. Martínez-Klimova E, Rodríguez-Peña K, Sánchez S. Endophytes as sources of antibiotics. *Biochem Pharmacol*. 2017; 134: 1–17. <https://doi.org/10.1016/j.bcp.2016.10.010> PMID: 27984002
95. Afzal I, Shinwari ZK, Sikandar S, Shahzad S. Plant beneficial endophytic bacteria: mechanisms, diversity, host range and genetic determinants. *Microbiol Res*. 2019; 221: 36–49. <https://doi.org/10.1016/j.micres.2019.02.001> PMID: 30825940
96. Akhter M, Wal Marzan L, Akter Y, Shimizu K. Microbial bioremediation of feather waste for keratinase production: an outstanding solution for leather dehairing in tanneries. *Microbiol insights*. 2020; 13: 1178636120913280. <https://doi.org/10.1177/1178636120913280> PMID: 32440139
97. Cimermancic P, Medema MH, Claesen J, Kurita K, Wieland Brown LC, Mavrommatis K, et al. Insights into secondary metabolism from a global analysis of bacterial biosynthetic gene clusters. *Cell*. 2014; 158: 412–421. <https://doi.org/10.1016/j.cell.2014.06.034> PMID: 25036635
98. Golinska P, Wypij M, Agarkar G, Rathod D, Dahm H, Rai M. Endophytic actinobacteria of medicinal plants: diversity and bioactivity. *Antonie Van Leeuwenhoek*. 2015; 108: 267–289. <https://doi.org/10.1007/s10482-015-0502-7> PMID: 26093915
99. Ribeiro CM, Cardoso EJBN. Isolation, selection and characterization of root-associated growth promoting bacteria in Brazil Pine (*Araucaria angustifolia*). *Microbiol Res*. 2012; 167: 69–78. <https://doi.org/10.1016/j.micres.2011.03.003> PMID: 21596540
100. Khamna S, Yokota A, Lumyong S. Actinomycetes isolated from medicinal plant rhizosphere soils: diversity and screening of antifungal compounds, indole-3-acetic acid and siderophore production. *World J Microbiol Biotechnol*. 2009; 25: 649–655.
101. Nain L, Yadav RC, Saxena J. Characterization of multifaceted *Bacillus* sp. RM-2 for its use as plant growth promoting bioinoculant for crops grown in semi arid deserts. *Appl soil Ecol*. 2012; 59: 124–135.
102. Maggini V, De Leo M, Mengoni A, Gallo ER, Miceli E, Reidel RVB, et al. Plant-endophytes interaction influences the secondary metabolism in *Echinacea purpurea* (L.) Moench: an in vitro model. *Sci Rep*. 2017; 7: 1–8.
103. Uche-Okereafor N, Sebola T, Tapfuma K, Mekuto L, Green E, Mavumengwana V. Antibacterial activities of crude secondary metabolite extracts from *Pantoea* species obtained from the stem of *Solanum mauritianum* and their effects on two cancer cell lines. *Int J Environ Res Public Health*. 2019; 16: 602. <https://doi.org/10.3390/ijerph16040602> PMID: 30791418
104. Badshah SL, Faisal S, Muhammad A, Poulson BG, Emwas AH, Jaremko M. Antiviral activities of flavonoids. *Biomed Pharmacother*. 2021; 140: 111596. <https://doi.org/10.1016/j.biopha.2021.111596> PMID: 34126315
105. Zakaryan H, Arabyan E, Oo A, Zandi K. Flavonoids: promising natural compounds against viral infections. *Arch Virol*. 2017; 162: 2539–2551. <https://doi.org/10.1007/s00705-017-3417-y> PMID: 28547385
106. Majdi H, Zar Kalai F, Yeddess W, Saidani M. Phenolic compounds as antiviral agents: An In-Silico investigation against essential proteins of SARS-CoV-2. *Nat Resour Hum Heal*. 2022; 2: 62–78. <https://doi.org/10.53365/nrhh/143085>
107. Verma VC, Prakash S, Singh RG, Gange AC. Host-mimetic metabolomics of endophytes: looking back into the future. *Advances in Endophytic Research*. Springer; 2014. pp. 203–218.
108. Roy S, Yasmin S, Ghosh S, Bhattacharya S, Banerjee D. Anti-infective metabolites of a newly isolated *Bacillus thuringiensis* KL1 associated with kalmegh (*Andrographis paniculata* Nees.), a traditional medicinal herb. *Microbiol insights*. 2016; 9: MBI-S33394.
109. Blin K, Shaw S, Steinke K, Villebro R, Ziemert N, Lee SY, et al. antiSMASH 5.0: updates to the secondary metabolite genome mining pipeline. *Nucleic Acids Res*. 2019; 47: W81–W87. <https://doi.org/10.1093/nar/gkz310> PMID: 31032519
110. Kautsar SA, Blin K, Shaw S, Navarro-Muñoz JC, Terlouw BR, van der Hooft JJJ, et al. MIBiG 2.0: a repository for biosynthetic gene clusters of known function. *Nucleic Acids Res*. 2020; 48: D454–D458. <https://doi.org/10.1093/nar/gkz882> PMID: 31612915
111. Tan X, Zhou Y, Zhou X, Xia X, Wei Y, He L, et al. Diversity and bioactive potential of culturable fungal endophytes of *Dysosma versipellis*; a rare medicinal plant endemic to China. *Sci Rep*. 2018; 8: 1–9.
112. Horng Y-B, Yu Y-H, Dybus A, Hsiao FS-H, Cheng Y-H. Antibacterial activity of *Bacillus* species-derived surfactin on *Brachyspira hyodysenteriae* and *Clostridium perfringens*. *AMB Express*. 2019; 9: 1–9.
113. Liu Y, Ding L, Fang F, He S. Penicillilactone A, a novel antibacterial 7-membered lactone derivative from the sponge-associated fungus *Penicillium* sp. LS54. *Nat Prod Res*. 2019; 33: 2466–2470. <https://doi.org/10.1080/14786419.2018.1452012> PMID: 29553833

114. Koumoutsis A, Chen X-H, Henne A, Liesegang H, Hitzeroth G, Franke P, et al. Structural and functional characterization of gene clusters directing nonribosomal synthesis of bioactive cyclic lipopeptides in *Bacillus amyloliquefaciens* strain FZB42. *Am Soc Microbiol*; 2004. <https://doi.org/10.1128/JB.186.4.1084-1096.2004> PMID: 14762003
115. Paniagua-Michel J, Olmos-Soto J, Ruiz MA. Pathways of carotenoid biosynthesis in bacteria and microalgae. *Microb carotenoids from Bact microalgae*. 2012; 1–12.
116. Umeno D, Tobias A, Arnold F. Evolution of the C30 Carotenoid Synthase CrtM for Function in a C40 Pathway. *J Bacteriol*. 2003; 184: 6690–6699. <https://doi.org/10.1128/JB.184.23.6690-6699.2002>
117. Hadden WL, Watkins RH, Levy LW, Regalado E, Rivadeneira DM, van Breemen RB, et al. Carotenoid composition of marigold (*Tagetes erecta*) flower extract used as nutritional supplement. *J Agric Food Chem*. 1999; 47: 4189–4194. <https://doi.org/10.1021/jf990096k> PMID: 10552789
118. Asker D, Awad TS, Beppu T, Ueda K. Screening, isolation, and identification of zeaxanthin-producing bacteria. *Microbial Carotenoids*. Springer; 2018. pp. 193–209.
119. Barredo J-L. *Microbial carotenoids from bacteria and microalgae*. Methods Protoc Humana Press New York, NY, USA. 2012; 5.
120. Hanif A, Zhang F, Li P, Li C, Xu Y, Zubair M, et al. Fengycin Produced by *Bacillus amyloliquefaciens* FZB42 Inhibits *Fusarium graminearum* Growth and Mycotoxins Biosynthesis. *Toxins*. 2019. <https://doi.org/10.3390/toxins11050295> PMID: 31137632
121. Beasley FC, Vinés ED, Grigg JC, Zheng Q, Liu S, Lajoie GA, et al. Characterization of staphyloferrin A biosynthetic and transport mutants in *Staphylococcus aureus*. *Mol Microbiol*. 2009; 72: 947–963. <https://doi.org/10.1111/j.1365-2958.2009.06698.x> PMID: 19400778
122. Doroghazi JR, Metcalf WW. Comparative genomics of actinomycetes with a focus on natural product biosynthetic genes. *BMC Genomics*. 2013; 14: 1–13.
123. Alvin A, Miller KI, Neilan BA. Exploring the potential of endophytes from medicinal plants as sources of antimycobacterial compounds. *Microbiol Res*. 2014; 169: 483–495. <https://doi.org/10.1016/j.micres.2013.12.009> PMID: 24582778
124. de Paula Nogueira Cruz F, Ferreira de Paula A, Nogueira CT, Marques de Andrade PH, Borges LM, Lacava PT, et al. Discovery of a Novel Lineage *Burkholderia cepacia* ST 1870 Endophytically Isolated from Medicinal *Polygala paniculata* Which Shows Potent In Vitro Antileishmanial and Antimicrobial Effects. *Int J Microbiol*. 2021;2021. <https://doi.org/10.1155/2021/6618559> PMID: 33679984
125. Maheshwari R, Bhutani N, Suneja P. Isolation and characterization of ACC Deaminase Producing Endophytic *Bacillus mojavensis* PRN2 from *Pisum sativum*. *Iran J Biotechnol*. 2020; 18: e2308. <https://doi.org/10.30498/IJB.2020.137279.2308> PMID: 33542934
126. Ahmad SJ, Zin NM, Mazlan NW, Baharum SN, Baba MS, Lau YL. Metabolite profiling of endophytic *Streptomyces* spp. and its antiplasmodial potential. *PeerJ*. 2021; 9: e10816. <https://doi.org/10.7717/peerj.10816> PMID: 33777509
127. Jeso V, Iqbal S, Hernandez P, Cameron MD, Park H, LoGrasso P V, et al. Synthesis of Benzoquinone Ansamycin-Inspired Macrocyclic Lactams from Shikimic Acid. *Angew Chemie Int Ed*. 2013; 52: 4800–4804. <https://doi.org/10.1002/anie.201301323> PMID: 23554224
128. Li J, Neubauer P. *Escherichia coli* as a cell factory for heterologous production of nonribosomal peptides and polyketides. *N Biotechnol*. 2014; 31: 579–585. <https://doi.org/10.1016/j.nbt.2014.03.006> PMID: 24704144